# Characteristics of intercontinental transport of tropospheric ozone from Africa to Asia

Han Han[1], Jane Liu[1,2], Huiling Yuan[1], Ye Zhu[1,3], Yue Wu[1], Yuhan Yan[4], Aijun Ding[1]

[1]School of Atmospheric Sciences, Nanjing University, Nanjing, China

[2]Department of Geography and Planning, University of Toronto, Toronto, Canada

[3]Shanghai Public Meteorological Service Centre, Shanghai, China

[4]Chinese Academy of Science, Institute of Atmospheric Physics, Beijing, China

*Correspondence to:* Jane Liu (janejj.liu@utoronto.ca)

**Abstract.** Based on 20-year simulations using a global chemical transport model, GEOS-Chem, and a trajectory model, HYSPLIT, the transport of ozone produced in the African troposphere to Asia is investigated. The study shows that the influence of African ozone on Asia varies largely in time and space. In the middle and upper troposphere, the inflow of African ozone to Asia peaks around 25°N, being the largest in boreal winter and early spring (>10 ppbv) and the lowest in boreal summer (<6 ppbv). In the lower troposphere, imported African ozone ranges 2-6 ppbv over Asia, being highest in boreal winter (~4 ppbv) and lowest in boreal fall (~2 ppbv). The seasonality of the transport mainly results from the seasonal swing of the Hadley circulation and the Intertropical Convergence Zone (ITCZ) in Africa and subtropical westerlies along the transport pathways. These meteorological conditions combined with the seasonality of ozone precursor emissions from various sources in Africa can modulate the influence of African ozone on Asia. Ozone from the northern hemispheric Africa accounts for over 70% of the total African ozone over Asia in most altitudes and seasons. The interhemispheric

transport of ozone from the southern hemispheric Africa is observed most evidently in boreal winter
over the Asian upper troposphere and in boreal summer over the Asian lower troposphere. The former is
facilitated by the convective divergence in the upper troposphere over the ITCZ in Africa, while the
latter is driven by the Somali jet. In boreal winter, the intensity of the ITCZ in Africa is positively
correlated with the interannual variation of imported African ozone over Asia, because a stronger ITCZ
can uplift more surface ozone and ozone precursors and enhance lightning $NO_x$ generation, resulting in
more African ozone transported to Asia.

## 1 Introduction

Tropospheric ozone is a major air pollutant, harmful to human health (Anenberg et al., 2010),
agricultural crops, and natural ecosystems (Hollaway et al., 2012; Lefohn et al., 2017). It also acts as a
greenhouse gas, whose global mean radiative forcing is about $0.4 \pm 0.2$ W/m$^2$ (Myhre et al., 2013). The
dominant source of tropospheric ozone is from the photochemical reactions in which volatile organic
compounds (VOCs) and carbon monoxide (CO) are oxidized in the presence of nitrogen oxides ($NO_x$)
(Lelieveld and Dentener, 2000). Transport of ozone from the stratosphere downward is another
important source of tropospheric ozone (Neu et al., 2014; Akritidis et al., 2016). Due to its relatively
long lifetime (days to weeks in the free troposphere), ozone can be transported over long distances
across continents, as seen in a wealth of observation evidence (Huntrieser et al., 2005; Lewis et al.,
2007; Rastigejev et al., 2010; Verstraeten et al., 2015). Consequently, tropospheric ozone in a region is
greatly influenced by ozone transport from upwind regions (Doherty et al., 2013; Derwent et al., 2015).
Therefore, intercontinental transport of ozone has been a significant issue to scientists, public, and
policymakers concerned with air quality and climate change (HTAP, 2010; Cooper et al., 2015; Doherty,
2015).

There have been numerous studies on the three major source-receptor relationships in the Northern

Hemisphere for ozone transport among Asia, North America, and Europe, which are trans-Pacific (Jaffe et al., 2003; Zhao et al., 2003; Cooper et al., 2010), trans-Atlantic (Wild et al., 1996; Cooper et al., 2002;

50    Guerova et al., 2006), and trans-Eurasian (Wild et al., 2004; Fiore et al., 2009; Li et al., 2014). The trans-Pacific transport from Asia to North America has been studied most because of high pollutant emissions in Asia and their efficient eastward export (Cooper et al., 2010, 2011, 2015; Verstraeten et al., 2015; Huang et al., 2017; Lin et al., 2017).

Transport of ozone to Asia from various source regions in the world has received some attention
55    recently (Holloway et al., 2008; Nagashima et al., 2010; Wang et al., 2011; Li et al., 2014; Zhu et al., 2016; Zhu et al., 2017b). Imported ozone, its seasonal variation, and spatial distribution depend on numerous processes, involving chemistry (Wild et al., 2004; Li et al., 2014), and meteorology in Asia, the source regions, and along the transport pathways. Previous studies illustrated the important role that meteorology plays in these processes (Sudo and Akimoto, 2007; Sekiya and Sudo, 2012, 2014; Zhu et
60    al., 2017b). Governed by the westerlies in the Northern Hemisphere, the influence of European and North American ozone is larger in higher latitudes than in lower altitudes of Asia (Wild et al., 2004; Holloway et al., 2008; Zhu et al., 2017b). The seasonal switch in Asian monsoonal winds significantly affects the seasonal variation of ozone transported to Asia (Nagashima et al., 2010; Wang et al., 2011; Zhu et al., 2017b). The Asian monsoon anticyclone (South Asian High, SAH) has remarkable effects on
65    the upper tropospheric ozone transport over Eurasia (Vogel et al., 2014; Garny and Randel, 2016).

Africa covers areas from the Northern Hemisphere to the Southern Hemisphere; around three quarters of the continent are located in the tropics. Comparing with other continents, Africa has the most frequent lightning (Albrecht et al., 2016) and the largest burned areas (Giglio et al., 2013). Over 70% of tropospheric ozone produced in Africa from natural and anthropogenic sources is exported out of Africa
70    (Aghedo et al., 2007), making African ozone an obvious influence on the global tropospheric ozone budget (Piketh and Walton, 2004; Thompson, 2004; Williams et al., 2009; Bouarar et al., 2011; Zare et

al., 2014). There have been a few studies on the transport of African ozone to some locations in Asia (Liu et al., 2002; Sudo and Akimoto, 2007; Lal et al., 2014). Liu et al. (2002) found that African outflow makes a contribution of about 10-20 ppbv to ozone in the middle and upper troposphere over Hong

75 Kong, southeast of China, during the November-April period. Sudo and Akimoto (2007) showed that there is a significant interhemispheric ozone transport from South America to Japan in the upper troposphere in conjunction with ozone export from northern Africa. Lal et al. (2014) reported that the ozone distribution over western India in the lower troposphere during the summer monsoon seasons is affected by long-range transport from the east coast of Africa. Nevertheless, questions still remain on

80 how and how much African ozone is transported to Asia, the transport pathways and their seasonality, as well as underlying mechanisms for the transport.

The Intertropical Convergence Zone (ITCZ), defined as the convergence of the trade winds, is one of the most prominent meteorological phenomena in the tropics (Waliser and Gautier, 1993; Žagar et al., 2011; Suzuki, 2011). ITCZ is a heat engine driving the ascending branch of the Hadley circulation

85 (Nicholson, 2009; Suzuki, 2011). ITCZ and its seasonality can significantly impact the meteorological conditions over Africa (Nicholson, 2009; Collier and Hughes, 2011; Suzuki, 2011). Characterized with deep and strong convection, the equatorial region between the ITCZ branches is a region with effective interhemispheric mixing (Avery et al., 2001). Meanwhile, the ITCZ can be a barrier to interhemispheric exchange in the lower troposphere (Raper et al., 2001). The convective divergence in the upper

90 troposphere over the ITCZ was proposed to be one of the primary mechanisms for the interhemispheric transport (Hartley and Black, 1995; Avery et al., 2001). Based on aircraft and satellite observations, an anti-correlation was found between ozone abundances and convective outflow over central American ITCZ region by Avery et al. (2010). Together with the Southeast Asian monsoon, the movement of the ITCZ can modulate pollution transport to Southeast Asia (Pochanart et al., 2003, 2004). In addition, the

95 ITCZ over western Africa is found to play a significant role in controlling the transport of Saharan

mineral dust to northern South America, modifying its air quality and climate (Piketh and Walton, 2004; Doherty et al., 2012, 2014; Rodríguez et al., 2015). However, the influences of the ITCZ on ozone transport from Africa to Asia have not been well understood.

In this study, a comprehensive investigation is made on the transport of African ozone to Asia through integrated numerical analysis of tagged tracer and trajectory simulations. African ozone here refers to ozone generated in the African troposphere below the tropopause from all natural and anthropogenic sources, as Sudo and Akimoto (2007) suggested that investigation of ozone production from both sources is necessary. Our specific objectives are (1) to characterize the seasonal variation of ozone transport from Africa to Asia, (2) to investigate the underlying mechanisms responsible for such seasonal variation, and (3) to explore a possible connection between the ITCZ and the interannual variation of imported African ozone over Asia. Our analysis is based on the simulations from a 3-dimensional global chemical transport model, GEOS-Chem (Bey et al., 2001a), for 20 years from 1987 to 2006 and simulations from a trajectory climatology for the same period from the Hybrid Single-Particle Lagrangian Integrated Trajectory model (HYSPLIT) (Draxler and Hess, 1998; Stein et al., 2015). In section 2, we describe the two models and the meteorological data used in this study. The validation of GEOS-Chem simulations is also presented in section 2. We address the first objective in section 3 and the second and third in section 4. Section 5 offers an overview of the processes involved in the transport of African ozone to Asia. Finally, the conclusions are drawn in section 6.

## 2 Methodology

### 2.1 The GEOS-Chem model and its validation

A global 3-dimensional chemistry transport model, GEOS-Chem (version v9-02) (Bey et al., 2001a, http://geos-chem.org), is employed to simulate the global ozone distributions and the source-receptor relationships between Africa and Asia. GEOS-Chem includes a detailed simulation of tropospheric $O_3$-

120    $NO_x$-hydrocarbon-aerosol. It is driven by assimilated meteorological data from the GEOS at NASA Global Modeling and Assimilation Office (GMAO). The model has been used extensively in studying pollution transport (Bey et al., 2001b; Koumoutsaris et al., 2008; Zhang et al., 2008; Liu et al., 2011; Wang et al., 2011; Ridder et al., 2012; Long et al., 2015; Jiang et al., 2016; Huang et al., 2017; Ikeda et al., 2017; Zhu et al., 2017a; Zhu et al., 2017b).

125    In this version of GEOS-Chem, the global anthropogenic emission inventories are from EDGAR 3.2 for $NO_x$, CO, $SO_x$ (Olivier and Berdowski, 2001) and RETRO for VOC emissions (Pulles et al., 2007), with the following regional inventories: the US Environmental Protection Agency National Emission Inventory 2005 (NEI05) for North America, the Cooperative Programme for Monitoring and Evaluation of the Long-range Transmission of Air Pollutants in Europe (EMEP) inventory for Europe (Vestreng
130    and Klein, 2002), Big Bend Regional Aerosol and Visibility Observational (BRAVO) Study Emissions Inventory for 1999 in Mexico (Kuhns et al., 2003), and the Criteria Air Contaminants (CAC) inventory for Canada. The emission inventories for China and SE Asia are based on Streets et al. (2003, 2006). Biofuel emission inventory is from Yevich and Logan (2003). Biomass burning and Biogenic emissions are from the GFED3 inventory (van der Werf et al., 2010) and MEGAN 2.1 (Guenther et al., 2012)
135    respectively. Lightning $NO_x$ emissions are calculated with the scheme of Allen et al. (2010) and the vertical distribution suggested by Ott et al. (2010).

    To investigate the influence of African ozone on Asia, we used the standard mode for tagged ozone simulation in GEOS-Chem (Wang et al., 1998; Fiore et al., 2002; Zhang et al., 2008). The simulation is driven by GEOS-4 meteorology, which uses the deep convection scheme of Zhang and McFarlane
140    (1995) and the shallow convection scheme of Hack (1994). The simulation covers a period from January 1986 to December 2006 (using 1986 for model spin-up) at $4^o$ latitude by $5^o$ longitude horizontal resolution with 30 vertical layers, 17 levels in the troposphere. Transport and chemical timesteps used in the study are 10 minutes and 20 minutes, respectively, as suggested by Philip et al. (2016). The tagged

ozone simulation calculates the contributions of the source regions to the receptor region using ozone
production rates and loss frequencies of odd oxygen defined in GEOS-Chem ($O_x=$
$O_3+NO_2+2NO_3+3N_2O_5+HNO_3+HNO_4+PAN+PMN+PPN$, Fiore et al., 2002; Zhang et al., 2008). Since
ozone accounts for most of $O_x$, we refer to ozone instead of $O_x$ for clarity. The ozone production rates
and loss frequencies were generated and archived from a full chemistry simulation before the tagged
simulation (Zhang et al., 2008, Liu et al., 2011). The source region, Africa, is defined as the region of
$35^oS$-$15^oN$, $20^oW$-$55^oE$ and $15^oN$-$35^oN$, $20^oW$-$30^oE$. Therefore, ozone produced in Africa below the
tropopause is tagged as a tracer. We further divided Africa into northern hemispheric Africa (NHAF)
and southern hemispheric Africa (SHAF) separated by the equator and thus added two more tracers. The
receptor region, Asia, is defined as the region of $5^oN$-$40^oN$, $60^oE$-$145^oE$. In the simulation, seasonal
variation of chemistry and meteorology are both considered. For the interannual variation, our purpose
is focused on the impact of meteorology on the transport of African ozone to Asia. Therefore, the
meteorology was set to vary from year to year, while a fixed chemistry was used for the 20-year
simulation, i. e., with the archived daily ozone production and loss data in 2005, similar to the
treatments in previous studies that examined the influences of meteorology on pollution transport (Liu
et al., 2011; Zhao et al., 2012; Sekiya and Sudo, 2014; Zhu et al., 2017b).

To quantify accurately the contribution of different sources to ozone abundances in a receptor region
using a numerical model, a good agreement between the model simulations and observations is required
(Cooper et al., 2015; Derwent et al., 2016). Although the GEOS-Chem simulations have been
extensively validated (Zhang et al., 2008; Liu et al., 2009; Wang et al., 2011; Kim et al., 2015; Zhu et al.,
2017a; Zhu et al., 2017b), we specifically validated the model in Africa for an enhanced confidence on
the model performance, using the ozonesonde measurements acquired from the World Ozone and
Ultraviolet Radiation Data Centre (WOUDC) (http://www.woudc.org/home.php). We selected three
ozonesonde stations at Santa Cruz in North Africa ($28.42^oN$, $16.26^oW$, 36 m), Nairobi in East Africa

(1.27$^o$S, 36,8$^o$E, 1745 m) and Irene in South Africa (25.91$^o$S, 28.21$^o$E, 1524 m). The ozonesonde

observations have been used in studies on African tropospheric ozone widely (Clain et al., 2009;

170   Thompson et al., 2012, 2014). Fig. 1 shows the vertical ozone profiles averaged from 1990 to 2003 for

Santa Crutz, from 1996 to 2006 for Nairobi, and from 1990 to 2006 for Irene by season. The

simulations and the observations exhibit good agreements. However, the model underestimates upper

tropospheric ozone in Nairobi in the four seasons and somewhat overestimates ozone near the surface in

Irene.

175

## 2.2 The HYSPLIT trajectory model

We use HYSPLIT_4 (Hybrid Single-Particle Lagrangian Integrated Trajectory, version 4) (Draxler and

Hess, 1998; Stein et al., 2015) forward trajectories to show the outflows from Africa. With powerful

computational capabilities, the HYSPLIT model is one of the most extensively used atmospheric

180   transport and dispersion models (Fleming et al., 2012). Meteorological inputs to HYSPLIT are the

NCEP reanalysis at a resolution of 2.5$^o$×2.5$^o$ (http://ready.arl.noaa.gov/archives.php). Six-day forward

trajectories were calculated from 1987 to 2006 four times a day (00, 06, 12 and 18 UTC) at four sites,

Cairo (31$^o$E, 30$^o$N, in North Africa), Abuja (7.4$^o$E, 9$^o$N, in West Africa), Dar es Salaam (39$^o$E, 6.8$^o$S, in

East Africa) and Johannesburg (28$^o$E, 26.2$^o$S, in South Africa). The level at 1.5 km, 5.5 km, and 11 km

185   are selected to represent the lower, middle and the upper troposphere, respectively. The results were

clustered for each month.

## 2.3 Meteorological data

The meteorological data include the NCEP/NCAR reanalysis I (Kalnay et al., 1996). The daily wind

190   fields are used to describe the climatology of atmospheric circulation during the study period from 1987

to 2006. The product is available on a 2.5$^o$×2.5$^o$ horizontal grid at 17 pressure levels from 1000 hPa to

10 hPa (https://www.esrl.noaa.gov/psd/data/gridded/data.ncep.reanalysis.html).

Additionally, the monthly Outgoing Longwave Radiation (OLR) data from NCAR at $2.5^o \times 2.5^o$ with temporal interpolation (Liebmann and Smith, 1996, https://www.esrl.noaa.gov/psd/data/gridded/ data.interp_OLR .html) are used to indicate the intensity of the convection over ITCZ. The dataset has been widely used for tropical studies on deep convection and rainfall (Mounier and Janicot, 2004).

## 3 Seasonal variation in imported African ozone over Asia

Because a substantial amount of ozone and ozone precursors are produced or emitted in Africa, tropospheric ozone in the other continents is largely influenced by ozone outflow from Africa (Williams et al., 2009; Zare et al., 2014). Fig. 2 shows seasonal variations of imported African ozone in the Asian troposphere, varying with latitude and altitude. The values are the 20-year means (1987-2006) from the GEOS-Chem simulation. The largest African influences appear in the Asian middle and upper troposphere, i.e., 2-16 ppbv at 500 and 700 hPa. African ozone in the Asian lower troposphere is reduced to between 2 to10 ppbv at 700 hPa throughout the year. Unlike imported European and North American ozone that influences Asia mostly over high altitudes (north of 30°N) (Wild et al., 2004; Holloway et al., 2008; Nagashima et al., 2010; Zhu et al., 2017b), imported African ozone prevails over lower latitudes, generally south to $40^o$N, considerably larger than European and North American ozone south of $30^o$N (Wild et al., 2004; Sudo and Akimoto, 2007; Zhu et al., 2017b). North of 50 $^o$N, African ozone influence is small, i.e., less than 4 ppbv and 2 ppbv, respectively, above and below the Asian middle troposphere. Seasonally, imported African ozone in the middle and upper troposphere peaks in March $25^o$N (~16 ppbv, Figs. 2a and 2b) and is at its minimum in July. Owing to the high radiative forcing efficiency, the change in ozone concentrations in the upper troposphere can impact climate more significantly than that in the lower troposphere (Lacis et al., 1990). Therefore, the influence of African ozone on the climate in southern Asia is likely larger than that of European and North American ozone

(Aghedo et al., 2007; Sudo and Akimoto, 2007). In the lower troposphere (Fig. 2c), between 10-40$^{o}$N, African ozone is high in boreal winter (6-10 ppbv), while south of 15$^{o}$N, African ozone peaks in boreal summer (~4 ppbv).

The strong seasonality of imported African ozone can also be shown vertically in Fig.3a, in which
220 imported African ozone is averaged over Asia. The fractional contribution of imported African ozone to ozone in Asia is shown in Fig. 3b. In the upper troposphere, imported African ozone is the most during February-May (>10 ppbv) and the least during July-September (<6 ppbv). Slightly different from the situation in the upper troposphere, imported Africa ozone in the Asian middle troposphere is at a maximum (>10 ppbv, 14% in the fractional contribution) from December to April and at a minimum
225 from June to September (~4 ppbv, 6% in the fractional contribution). In the lower troposphere, imported African ozone is the largest in boreal winter (~4 ppbv, 8% in the fractional contribution), lowest in boreal fall (~2 ppbv, 5% in the fractional contribution). Seasonal-altitude variations of imported ozone from NHAF and SHAF over Asia and the fractional contributions of NHAF and SHAF ozone to the total imported African ozone are shown in Fig. 4. Ozone from NHAF accounts for over 70% of the total
230 imported African ozone in the Asian tropospheric column throughout the year, except for in the upper troposphere in boreal winter and the lower troposphere in boreal summer. The summertime transport of SHAF ozone to the Asian lower troposphere is also shown in a summer maximum of African ozone in Fig.2c (~4 ppbv at 700 hPa, south of 15$^{o}$N). This was also reported by Lal et al. (2014), who attributed it to ozone transport from the Indian Ocean from the east coast of Africa.

235 As African ozone mainly peaks in the Asian middle and upper troposphere, the horizontal distributions of African ozone at 400 hPa in January, April, July, and October overlaid with winds are shown in Fig. 5 to further illustrate its seasonality and transport pathways. Driven by the upper tropospheric easterly jet around the equator (Diedhiou et al., 1999), high African ozone appears across the Atlantic, reaching the South America throughout the year. The westward transatlantic routes from

240  northern Africa are built by the easterly waves (Jones et al., 2003; Mari et al., 2008; Ben-Ami et al.,

2009). In boreal winter, near the northern and southern borders of Africa, African ozone can be

transported for a long distance along the subtropical westerly jets in the two hemispheres, reaching the

western Pacific in the Northern Hemisphere and across Australia in the Southern Hemisphere,

respectively. In boreal summer, the northern subtropical westerlies and tropical easterlies shift to their

245  most northern positions; less African ozone can be transported to Asia than in the other seasons.

However, around $40^o$N, the amount of African ozone being transported to Asia is similar to the other

season (Fig. 2a).

**4 Possible mechanisms for the transport of African ozone to Asia**

250  In this section, we analyze the transport pathways from Africa to Asia and associated underlying

mechanisms so to cast some light on the spatial and seasonal variations in imported African ozone over

Asia presented in section 3. Since Africa covers areas in both Northern and Southern Hemispheres with

a large portion in the tropics, the atmospheric circulation over Africa experiences obvious seasonal

changes induced by the seasonality of the ITCZ and the Hadley cell (Nicholson and Grist, 2003;

255  Nicholson, 2008, 2009; Žagar et al., 2011; Suzuki, 2011). African ozone precursors are mainly from

biogenic sources, biomass burning, and lightning $NO_x$ (Piketh and Walton, 2004; Thompson, 2004;

Aghedo et al., 2007; Giglio et al., 2013; Monks et al., 2015). The seasonalities of emissions from

biogenetic sources, biomass burning, lightning, and anthropogenic sources in Africa are characterized

rather differently from the other continents (Williams et al., 2009; Guenther et al., 2012; Giglio et al.,

260  2013; Albrecht et al., 2016).

**4.1 The ITCZ and ozone precursor emissions over Africa**

Referred to Nicholson (2009), Suzuki (2011), and Žagar et al. (2011), the mean positions of the ITCZ in

Africa in the four seasons are approximately illustrated in Figs. 6a-6d. The seasonal migration of the

265    ITCZ between latitudes is a robust phenomenon and varies with longitude (Nicholson, 2009; Suzuki, 2011). The latitudinal shift is wider in eastern Africa than in western Africa (Figs. 6a-6d). From boreal winter to summer, the center of the ITCZ swings from $10^{o}$N to $20^{o}$N in western Africa (Figs. 6a-6d), while in eastern Africa between $10^{o}$E and $40^{o}$E, ITCZ shifts between ~$10^{o}$S in boreal winter and ~$20^{o}$N in boreal summer (Figs. 6a-6d).

270    African ozone and its seasonality depend heavily on biogenic emissions, moderately on biomass burning and lightning emissions, and weakly on anthropogenic emissions. The anthropogenic emissions are small and have weak seasonality (Aghedo et al., 2007; Williams et al., 2009). The spatial distributions of isoprene emissions from biogenic sources, CO emissions from biomass burning, and $NO_x$ emissions from lightning are shown by season in Fig. 6. The normalized seasonal variations of

275    these emissions averaged over Africa, NHAF and SHAF are shown in Fig. 7. The emission data are from the emission inventories in GEOS-Chem described in section 2.1. The normalized value equals to the original value minus the annual mean and then divided by the standard deviation.

As isoprene ($C_5H_8$) is the dominant non-methane volatile organic compound (NMVOC) emitted by vegetation (Marais et al., 2012) and biogenic isoprene emissions in Africa account for about 65% of the

280    African upper troposphere ozone enhancement (Aghedo et al., 2007), isoprene emissions are shown in Figs. 6a-6d as a representative ozone precursor from biogenic sources. The maximum biogenic isoprene emissions are over central African rainforests throughout the year (Fig. 6a-6d). The seasonal cycle of biogenic isoprene over Africa peaks in boreal spring and fall (Fig. 7a). Plenty of non-methane VOCs, which may have relatively long lifetimes (such as methanol) or effective storage of $NO_x$ (such as PAN),

285    are emitted from biogenic sources that can be uplifted by strong convection (Tie et al., 2003). Consequently, the contribution of biogenic emissions to ozone in the African upper troposphere is larger than biomass burning and anthropogenic emissions (Aghedo et al., 2007; Zare et al., 2014).

In boreal winter, fires in Africa are active in the Northern Hemisphere between 0-10$^{o}$N and 15$^{o}$W to 40$^{o}$E (Sauvage et al., 2005). From boreal winter to fall, biomass burning regions shift southward from central Africa to southern Africa (Fig. 6, 2$^{nd}$ row, also see van der Werf et al., 2010; Giglio et al., 2013). In the Southern Hemisphere, fires are most active in boreal summer from the equator to 20$^{o}$S. Therefore, the regional CO emissions from biomass burning peak in boreal winter in NHAF and in boreal summer in SHAF (Fig. 7b). Aghedo et al. (2007) stated that biomass burning has the largest impact on surface ozone in the vicinity of the African burning regions during the burning seasons.

In Africa, lightning NO$_x$ is produced mostly in the middle to upper troposphere (Figs. 6i-6p, also see Pickering et al., 1998). Miyazaki et al. (2014) estimated that the altitude where the annual lightning NO$_x$ emission maximizes is 11 km for northern Africa and 9.36 km for southern Africa. Therefore, lightning emissions mainly enhance ozone in the African middle and upper troposphere (Aghedo et al., 2007). Ascribe to the high efficiency of deep moist convection, frequent lightning activities occur in the ITCZ (Christian et al., 2003; Avila et al., 2010). Collier and Hughes (2011) suggested that the peak lightning activities are generally located on the southern border of the ITCZ in Africa. The seasonality of the locations for high lightning NO$_x$ emission clearly shows the influence of the solar declination and the ITCZ over Africa (Collier and Hughes, 2011). When the ITCZ reaches to its northernmost position in boreal summer (Fig. 6c), lightning NO$_x$ emission over the NHAF becomes the highest (Figs. 6, 7c and 7d). Similarly, the lightning NO$_x$ emission over the SHAF peaks in boreal winter (Figs. 6, 7c and 7d).

**4.2 Analysis of the transport pathways based on GEOS-Chem simulations**

Fig. 8 shows the latitude-altitude cross sections of African ozone and wind fields averaged from 0 to 40$^{o}$E. Fig. 9 is the same as Fig. 8 but for the longitude-altitude cross sections averaged from 25$^{o}$N to 35$^{o}$N. In Fig. 10, vertical distributions of African ozone fluxes along the western border and eastern border of Asia are shown by season. Apparently, the inflow fluxes are larger than the outflow fluxes

throughout the year. Controlled by the northern subtropical westerly jet, imported African ozone fluxes peak in the upper troposphere. The latitudes where African ozone flux peak vary with the seasonal swing of the northern subtropical westerlies.

315   In boreal winter, deep convection, strong convergence in the lower troposphere can be seen from $10^{o}$S to $20^{o}$S (Fig. 8a), indicating the position of the ITCZ in the Southern Hemisphere. The two cells of the Hadley circulation are clearly shown as well. Due to frequent lightning activities, the region with high ozone appears over the ITCZ in the African middle and upper troposphere in the Southern Hemisphere. In the lower troposphere, ozone concentrations are high from the equator to $10^{o}$N,

320   resulting from high biomass burning emissions as discussed in section 4.1 (Aghedo et al., 2007). This ozone is uplifted (Fig. 8a, 0-$10^{o}$N) by the ITCZ in the Northern Hemisphere (Figs. 6a and 6e). Driven by the Hadley cell, ozone in NHAF is transported equatorward in the lower troposphere, upward over the ITCZ, poleward in the middle and upper troposphere. The northward outflow in the middle and upper troposphere gradually becomes weaker and weaker between 15-$30^{o}$N (Fig. 8a). Eventually,

325   carried by the subtropical westerlies, African ozone is transported eastward to Asia (Fig. 9a, also see Fig. 12a in section 4.4). Consequently, the contribution of African ozone to Asia becomes the highest in the middle and upper troposphere (see Figs. 2b and 3a for ozone concentrations, and Fig. 10a for inflow ozone flux). During the season, the divergence outflow in the Southern Hemispheric upper troposphere carries African ozone (Fig. 8a, 500-200 hPa, 10-20°S) to the Asian upper troposphere, contributing to 2-

330   3 ppbv ozone, which is 30% of the total imported African ozone over Asia (Figs. 4c and 4d).

In boreal spring, a region with high ozone concentrations (>40 ppbv) appears in higher altitudes and extends to a larger area in the middle and upper troposphere than in boreal winter (Figs. 8b and 9b) mainly due to the highest biogenic emissions in the NHAF (section 4.1, Figs. 6b and 7a). The region is also further north than in boreal winter under the influence of seasonal migration in the locations of the

335   ITCZ and consequently the lightning. Ozone in the African lower troposphere becomes lower than in

boreal winter, likely due to weaker biomass burning activities in the central Africa (Duncan et al., 2003). In general, the pathways for African ozone to be transported to Asia in boreal spring are similar to those in winter (Figs. 5a vs 5b, 8a vs 8b, 9a vs 9b, 10a vs 10b). In the upper troposphere, however, more ozone is transported to Asia in boreal spring than in boreal winter (Fig. 3a), mainly due to the seasonal

340  increase of biogenic emissions (Fig. 7a).

In boreal summer, African ozone in the lower troposphere peaks from ~15$^{o}$S to the equator (Fig. 8c), corresponding to the biomass burning emissions (Figs. 6g and 7b). However, because the center of the ITCZ shifts to ~20$^{o}$N over the Sahara (Fig. 6c), ozone generated from biogenic emissions is uplifted less effectively than in the other seasons (Fig. 8c vs 8a, 8b, and 8d). Consequently, ozone in the African

345  middle and upper troposphere south of 15$^{o}$N is lower than in the other seasons (Fig. 8c). However, resulting from the northward migration of lightning activities, ozone in the middle and upper troposphere north of 15$^{o}$N is higher than in the other seasons (Fig. 8c). The transport of African ozone to Asia in boreal summer differs from that in boreal winter. In boreal summer, the updrafts over the Tibetan Plateau are strong (Fig. 9c), which serves as a heat source for the Asian summer monsoon (Wu

350  et al., 2012, 2015) and blocks the transport of African ozone to Asia (Fig. 9c). Furthermore, the northern westerly jet moves northward to around 40$^{o}$N (Huang et al., 2012). The tropical easterlies also shift northward along (Fig. 5c) and further prevent African ozone from reaching Asia between 10$^{o}$N and 30$^{o}$N above the lower troposphere (see Figs. 2a-2d, and 3a-3b for imported ozone concentrations, Fig. 10c for inflow ozone flux).

355  In boreal autumn, the locations of the ITCZ and the Hadley cell are similar to these in boreal spring (Figs. 8b vs 8d). Ozone in the African middle troposphere is higher in boreal autumn than in boreal spring, attributed to stronger lightning NO$_x$ emission (Figs. 7c and 7d). However, because of the weaker zonal winds (Figs. 9b vs 9d), the ozone inflow to Asia is smaller than in spring (Figs. 10b vs 10d).

Overall, the influence of African ozone on the Asian middle and upper troposphere is mainly

360    attributed to ozone transport driven by the Hadley circulation and subtropical westerlies. The

seasonality of the ITCZ, the Hadley cell, and the westerlies can greatly influence the seasonality of the

pathways of ozone transport from Africa to Asia.

### 4.3 Interhemispheric transport of ozone from the SHAF to Asia

365    In the upper troposphere, the horizontal distribution of SHAF ozone at 200 hPa in January is shown in

Fig. 11a. SHAF ozone in Asia is 2-3 ppbv along 60°N-150°E between 0-30°N (Fig. 11a). Because of the

ITCZ and the Hadley circulation, a part of SHAF ozone is inter-hemispherically transported to the

Northern Hemisphere (Fig. 8a). Then, driven by northern subtropical westerly jet, this ozone can finally

reach Asia (Fig. 11a). Over Asia, ozone from SHAF is the largest in boreal winter than in the other

370    seasons in the upper troposphere, while in the lower troposphere, it is the largest in summer than in the

other seasons (Figs. 4c and 4d). Fig. 11b shows SHAF ozone in July at 925 hPa, with concentrations of

2-6 ppbv over the Arabian Sea and the west coast of the Indian subcontinent. This ozone is transported

to India in boreal summer by the Somalia cross-equatorial flow (Fig. 11b), which is the strongest

seasonal cross-equatorial flow in the lower troposphere (Halpern and Woiceshyn, 1999, 2001). This is

375    the reason for the summer maximum of African ozone (~4 ppbv) over the Asian lower troposphere

south of 15°N (Fig. 2c). This transport is also captured in Fig. 10c as the influx of Africa ozone in the

Asian lower troposphere south of 15°N.

### 4.4 Analysis of the transport pathways based on trajectory statistics

380    In this section, we use six-day forward trajectories to further analyze the pathways for ozone transport

from Africa to Asia. Fig. 12 shows the clustered six-day forward trajectories during 1987-2006 starting

from Cairo (31°E, 30°N), Abuja (7.4°E, 9°N), Dar es Salaam (39°E, 6.8°S), and Johannesburg (28°E,

26.2°S) in the lower, middle and upper troposphere, respectively. The four sites are chosen for different

latitudes in Africa.

385    In boreal winter, in NHAF, ~40% of the 6-days trajectories in the lower troposphere from Cairo flow

to higher latitudes in Asia (Fig. 12c). In the middle troposphere, ~74% trajectories from Cairo reach

Asia along the northern subtropical westerlies (Fig. 12b). Approximately, 10% trajectories from Abuja

reach Asia following a pathway of upward along the northern Hadley cell and then eastward along the

northern subtropical westerlies (Fig. 12b). In the upper troposphere, African ozone can be transported to

390    Asia fast and with longer distances within 6 days (Fig. 12a). After reaching Asia (across 60°E), most of

the trajectories in the middle and upper troposphere move downwards along the westerlies (Figs. 12a

and 12b). Driven by the northern subtropical westerly jet, 98% trajectories from Cairo and about 41%

trajectories from Abuja can reach Asia (Fig. 12a). Toward to further south, Dar es Salaam is mainly

under the influence of the tropical easterlies and the south subtropical westerlies in the lower and

395    middle troposphere so that the trajectories from this site are either westwards or eastwards along the

westerlies in the Southern Hemisphere (Figs. 12b and 12c). However, in the upper troposphere, about 25%

trajectories at the site flow to Asia (Fig. 12a) due to the convective divergence over the ITCZ. At

Johannesburg in the southern Africa, nearly no trajectories can reach Asia (Figs. 12a-12c).

In boreal summer, induced by the northward shift of the northern subtropical westerlies (~40°N),

400    fewer trajectories reach Asia than in winter (Figs. 12d-12f). Because of the northward shift of the

Hadley cell and the tropical easterlies, trajectories from Abuja travel westward in the middle and upper

troposphere, while in the lower troposphere, the trajectories run around locally (Figs. 12d, 12e, and 12f).

Similar to winter, no trajectories from Johannesburg reach Asia because of the southern location of the

site (Figs. 12d, 12e, and 12f). However, at Dar es Salaam in east Africa, there are ~14% trajectories in

405    the lower troposphere that travel toward India (Figs. 12e and 12f) under the influence of Somali jet

(Halpern and Woiceshyn, 1999, 2001; Lal et al., 2014). The Somali jet can transport ozone from the east

coast of Africa to Asia, resulting in a summer maximum of African ozone over the Asian lower

troposphere south of 15°N (Fig. 2c for ozone concentration, and Fig 10c for the ozone inflow flux).

Overall, the analysis of the trajectory statistic agrees well with the GEOS-Chem simulations discussed

410    in section 4.2.

## 4.5 Influences of the ITCZ on the interannual variation of African ozone transport to Asia in boreal winter

As known, the deep convection along the ITCZ can carry ozone precursors from biogenic, biomass

415    burning, and anthropogenic emissions to upper levels. The ITCZ is also a zone with large lightning

activities. The convective divergence in the upper troposphere over the ITCZ plays a significant role in

ozone outflow and the interhemispheric transport between SHAF and NHAF. Therefore, the ITCZ can

impact meteorology in Africa (Sultan and Janicot, 2000; Xie, 2004; Hu et al., 2007; Collier and Hughes,

2011; Suzuki, 2011) and the seasonality of ozone precursor emissions (for example, $NO_x$ from

420    lightning). To explore the role that the ITCZ plays in ozone transport from Africa to Asia, we use the

OLR data as a proxy for convective activity in the tropics to describe the intensity of ITCZ, similar to

previous studies (Waliser et al., 1993; Mounier and Janicot, 2004; Fukutomi and Yasunari, 2013, 2014).

According to Waliser et al. (1993) and Fukutomi and Yasunari (2013), the number of the grid points

with OLR $\leq 260$ W/m$^2$ in the region of 15$^o$W-45$^o$E, 20$^o$S-20$^o$N can indicate the intensity of the

425    convection over the ITCZ in Africa.

Fig. 13 shows time series of ozone from Africa, NHAF and SHAF, averaged over Asia, against the

intensity of the ITCZ over Africa (after normalization, i.e., the original value minus the mean that is

divided by the standard deviation) in January from 1987 to 2006. The anomalies of imported ozone

from SHAF are quite small in the lower and middle troposphere (Fig. 4), so the time series is not shown.

430    Positive correlations are found between the intensity of the ITCZ and anomalies of African ozone over

Asia, with the correlation coefficient (r) being 0.61, 0.46, and, 0.64 for the Asian lower (975 hPa),

middle (600 hPa) and upper (200 hPa) troposphere, respectively, all statistically significant at the 95% level (p<0.05). Significant correlations are also found for NHAF and SHAF ozone in the upper troposphere (Fig. 13a). In boreal winter, the center of the ITCZ is located in the upper region of biogenic and biomass burning emissions (Figs. 6a and 6e). When the intensity of the African ITCZ is stronger, more ozone and ozone precursors are uplifted to the middle and upper troposphere and transported poleward and then eastward to Asia by the northern subtropical westerlies (Figs. 12a-12c). Additionally, driven by the enhanced convective divergence over the ITCZ, the interhemispheric transport from SHAF increases in the upper troposphere (Figs. 8a and 13a). Consequently, transport of ozone from Africa to Asia increases in the middle and upper troposphere. At the same time, carried by the downdrafts from Asian winter monsoon (Figs. 9a, 12a-12c), more ozone is transported to the surface in Asia (Zhu et al., 2017b).

## 5 An overview on the transport of African ozone to Asia

The processes discussed in section 4 on the transport of African ozone to Asia can be briefly summarized for boreal winter (Fig. 14a) and boreal summer (Fig. 14b), respectively, from perspectives of both the atmospheric circulations (Xie, 2004; Mari et al., 2008; Nicholson, 2009; An et al., 2015; Ding et al., 2015; Li et al., 2016; Nützel et al., 2016) and emissions of ozone precursors (Aghedo et al., 2007; Marais et al., 2012; Giglio et al., 2013; Miyazaki et al., 2014; Zare et al., 2014; Albrecht et al., 2016).

During boreal winter, the Hadley cell and the northern subtropical westerlies build the transport pathways from Africa to Asia. Formed at the ascending branch of the Hadley circulation, the location of the ITCZ over Africa shows different characteristics in Africa west of 10°E and Africa east of 10°E (Nicholson, 2009). Over the ITCZ, a great amount of latent heat is released by deep convection, which drives the ascending branch of the Hadley circulation (Xie, 2004). The biomass burning emissions are

mainly in the Northern Hemisphere (Fig. 6e), which contributes to the production of a significant amount of African ozone in the lower troposphere (Fig. 8a, also see Mari et al., 2008). The ozone precursors can be carried upward from the surface to the upper layers by the rising branch of the Hadley circulation.

460     In the African middle and upper troposphere, vigorous convection within ITCZ clouds results in strong thunderstorms, accompanied with much lightning (Avila et al., 2010). Based on the C-shaped vertical profile of the lightning-generated $NO_x$, lightning activities contribute to the generation of a large proportion of ozone in the African middle and upper troposphere (Fig. 8a, also see Pickering et al., 1998; Miyazaki et al., 2014). Then ozone generated from chemical reactions and convection uplifting is

465     transported poleward by the convective divergence over the ITCZ and downward by the descending branch of the Hadley cell. The northern subtropical westerlies carry African ozone to Asia in the middle and upper troposphere. Overall, in boreal winter, African ozone is mainly produced from biogenic and lightning sources (Aghedo et al., 2007; Zare et al., 2014) and is transported to Asia mostly in the middle and upper troposphere, governed by the northern Hadley cell and subtropical westerlies.

470     In boreal summer, the ITCZ and the Hadley circulation move northward in response to the solar heating to the Northern Hemisphere. The African easterly jet, topical easterly jet and northern subtropical westerly jet all shift northward as well. However, the fire areas shift southward to the Southern Hemisphere (Clain et al., 2009; Giglio et al., 2013). Therefore, the ITCZ can facilitate lightning $NO_x$ production in NHAF but uplifts little ozone generated from biomass burning. In the

475     upper troposphere, transport of African ozone to Asia is hampered by the SAH, a prevailing weather system over Eurasia in boreal summer (Nützel et al., 2016). The updrafts associated with SAH prevent African ozone from reaching Asia at low latitudes (<30°N) (Fig. 9c). In the meantime, the easterlies prevail south of 30°N so to block African ozone from reaching Asia. Overall, both the meteorology and emissions in boreal summer weaken the transport of African ozone to Asia in the middle and upper

480   troposphere. Noticeably, the Asian summer monsoon (Zhang et al., 2002; Ding et al., 2005) is in favor

of transport of African ozone to Asia in the lower troposphere. Located north to the enhanced

Mascarene Anticyclone, on the east coast of Somali, Somali cross-equatorial flow served as an essential

component of the Asian monsoon system (Joseph and Sijikumar, 2004). Peaked at 925 hPa (Zhu, 2012),

the Somali jet carries ozone in eastern Africa to India in the lower troposphere (Figs. 10c and 11b).

485

**6 Conclusions**

The transport of ozone originated in the African troposphere to Asia is investigated through the analysis

of the simulations using a global chemical transport model, GEOS-Chem, and a trajectory model,

HYSPLIT. This study shows that imported African ozone varies greatly with latitude, longitude, and

490   altitude in the Asian troposphere, also with strong seasonality. In the Asian upper troposphere, imported

African ozone is the largest during February-May (>10 ppbv) and the lowest during July-September (<6

ppbv). In the middle troposphere, imported African ozone is at a maximum from December to April

(>10 ppbv) and at a minimum from June to September (~4 ppbv), slightly different from the seasonality

in the upper troposphere. In the lower troposphere, the African influence is small (<6 ppbv), with a

495   maximum from December to February (>6%) and a minimum from September to November (<5%).

Overall, the maximum influence of African ozone is in boreal winter and early spring in the middle and

upper troposphere of southern Asia ($5^o$N-$40^o$N). Ozone from NHAF makes up over 80% of the total

imported African ozone in most seasons and layers in Asia, except over the upper troposphere in boreal

winter and over the lower troposphere in summer, when the interhemispheric transport of ozone from

500   SHAF becomes stronger than in the other seasons at the same layers.

The underlying mechanisms for these seasonal variations in the transport of African ozone to Asia are

explored. In boreal winter, facilitated by ITCZ, ozone produced from its precursors from biogenic and

biomass burning sources can be efficiently lifted up to high layers. The uplifted African ozone is

transported poleward by the Hadley circulation in the upper troposphere and then eastward by the

505    subtropical westerlies in the middle and upper troposphere. The convective divergence over the ITCZ

(the poleward branch of the Hadley circulation) in the Southern Hemisphere promotes the

interhemispheric transport of SHAF ozone, resulting in a contribution of SHAF ozone of 2-3 ppbv in

the upper troposphere, larger than in the other seasons. Under the influence of both the Hadley

circulation and subtropical westerlies, African ozone peaks mainly in the Asian middle and upper

510    troposphere. In boreal summer, as the northern westerlies shift northward, African ozone is mostly

transported to the Asian upper troposphere around $40^{o}$N. In the lower troposphere, the Somali jet serves

as another important pathway for the interhemispheric transport of SHAF ozone, carrying ozone from

eastern Africa to India and thus forming a summer African ozone maximum in the lower troposphere

over latitudes south of $15^{o}$N.

515    The interannual variation in African ozone transport to Asia is greatly influenced by the intensity of

the ITCZ in boreal winter. Positive correlations are found between the intensity of the ITCZ in Africa

and the interannual variations of imported African ozone over Asia in various layers (r = 0.64 at 200 hPa,

r = 0.46 at 600 hPa, and r = 0.61 at 975 hPa). Greatly influenced by the proximity of the ITCZ to the

biogenic, biomass burning and anthropogenic emissions, the uplifting of ozone and its precursors from

520    the surface to higher altitudes is much more effective in boreal winter than in boreal summer. The

stronger the ITCZ in Africa is, the more ozone and its precursors from the surface emissions can be

uplifted. In the meanwhile, lightning $NO_x$ is produced in the middle and upper troposphere. Additionally,

the convective divergence over the ITCZ in the upper troposphere is enhanced, resulting in increased

interhemispheric transport from SHAF. Consequently, more African ozone can be transported to Asia by

525    the subtropical westerlies in the middle and upper troposphere.

*Acknowledgments.* We gratefully acknowledge that the GEOE-Chem model has been developed and managed by the Atmospheric Chemistry Modeling Group at Harvard University. The HYSPLIT (Hybrid Single-Particle Lagrangian Integrated Trajectory Model) model is developed by NOAA Air Resources Laboratory, driven by the NCEP reanalysis data provided by NOAA/OAR/ESRL PSD, Boulder, Colorado, USA. The ozone sounding data were obtained from the World Ozone and Ultraviolet Radiation Data Center (http://www.woudc.org) under the World Meteorological Organization. This research is supported by the Natural Science Foundation of China (41375140) and by the Chinese Ministry of Science and Technology under the National Key Basic Research Development Program (2014CB441203, 2016YFA0600204) and the Natural Science Foundation of China (91544230).

530

## References

Aghedo, A. M., Schultz, M. G., and Rast, S.: The influence of African air pollution on regional and global tropospheric ozone, Atmos. Chem. Phys., 7, 1193-1212, doi:10.5194/acp-7-1193-2007, 2007.

Akritidis, D., Pozzer, A., Zanis, P., Tyrlis, E., Škerlak, B., Sprenger, M., and Lelieveld, J.: On the role of tropopause folds in summertime tropospheric ozone over the eastern Mediterranean and the Middle East, Atmos. Chem. Phys., 16, 14025-14039, doi:10.5194/acp-16-14025-2016, 2016.

Albrecht, R. I., Goodman, S. J., Buechler, D. E., Blakeslee, R. J., and Christian, H. J.: Where are the lightning hotspots on Earth?, Bull. Amer. Meteor. Soc., 97, 2051-2068, doi:10.1175/BAMS-D-14-00193.1, 2016.

Allen, D., Pickering, K., Duncan, B., and Damon, M.: Impact of lightning NO emissions on North American photochemistry as determined using the Global Modeling Initiative (GMI) model, J. Geophys. Res., 115, D22301, doi:10.1029/2010JD014062, 2010.

An, Z., Wu, G., Li, J., Sun, Y., Liu, Y., Zhou, W., Cai, Y., Duan, A., Li, L., Mao, J., Cheng, H., Shi, Z., Tan, L., Yan, H., Ao, H., Chang, H., Feng, J.: Global Monsoon Dynamics and Climate Change, Annu. Rev. Earth Planet. Sci., 43, 29–77, doi:10.1146/annurev-earth-060313-054623, 2015.

Anenberg, S. C., Horowitz, L. W., Tong, D. Q., and West, J. J.: An estimate of the global burden of anthropogenic ozone and fine particulate matter on premature human mortality using atmospheric modeling, Environ. Health. Persp., 118, 1189-1195, doi:10.1289/ehp.0901220, 2010.

Avery, M., Westberg, D., Fuelberg, H., Newell, R., Anderson, B., Vay, S., Sachse, G., and Blake, D.: Chemical transport across the ITCZ in the central Pacific during an El Nino-Southern Oscillation cold phase event in March-April 1999, J. Geophys. Res., 106, 32539-32553, doi:10.1029/2001JD000728, 2001.

Avery, M., Twohy, C., McCabe, D., Joiner, J., Severance, K., Atlas, E., Blake, D., Bui, T., Crounse, J., and Dibb, J.: Convective distribution of tropospheric ozone and tracers in the Central American ITCZ region: Evidence from observations during TC4, J. Geophys. Res., 115, D00J21, doi:10.1029/2009JD013450, 2010.

Avila, E. E., Bürgesser, R. E., Castellano, N. E., Collier, A. B., Compagnucci, R. H., and Hughes, A. R.: Correlations

between deep convection and lightning activity on a global scale, J. Atmos. Sol-Terr. Phy., 72, 1114-1121,

560     doi:10.1016/j.jastp.2010.07.019, 2010.

Ben-Ami, Y., Koren, I., and Altaratz, O.: Patterns of North African dust transport over the Atlantic: winter vs. summer, based

on CALIPSO first year data, Atmos. Chem. Phys., 9, 7867-7875, doi:10.5194/acp-9-7867-2009, 2009.

Bey, I., Jacob, D. J., Logan, J. A., and Yantosca, R. M.: Asian chemical outflow to the Pacific in spring: Origins, pathways,

and budgets, J. Geophys. Res., 106, 23073-23095, doi:10.1029/2001jd000807, 2001a.

565     Bey, I., Jacob, D. J., Yantosca, R. M., Logan, J. A., Field, B. D., Fiore, A. M., Li, Q., Liu, H. Y., Mickley, L. J., and Schultz,

M. G.: Global modeling of tropospheric chemistry with assimilated meteorology: Model description and evaluation, J.

Geophys. Res., 106, 23073-23095, doi:10.1029/2001jd000806, 2001b.

Bouarar, I., Law, K. S., Pham, M., Liousse, C., Schlager, H., Hamburger, T., Reeves, C., Cammas, J.-P., Nédélec, P., and

Szopa, S.: Emission sources contributing to tropospheric ozone over Equatorial Africa during the summer monsoon,

570     Atmos. Chem. Phys., 11, 13395-13419, doi:10.5194/acp-11-13395-2011, 2011.

Christian, H. J., Blakeslee, R. J., Boccippio, D. J., Boeck, W. L., Buechler, D. E., Driscoll, K. T., Goodman, S. J., Hall, J. M.,

Koshak, W. J., and Mach, D. M.: Global frequency and distribution of lightning as observed from space by the Optical

Transient Detector, J. Geophys. Res., 108, ACL 4-1-ACL 4-15, doi:10.1029/2002JD002347, 2003.

Clain, G., Baray, J. L., Delmas, R., Diab, R., Bellevue, J. L. D., Keckhut, P., Posny, F., Metzger, J. M., and Cammas, J. P.:

575     Tropospheric ozone climatology at two Southern Hemisphere tropical/subtropical sites, (Reunion Island and Irene, South

Africa) from ozonesondes, LIDAR, and in situ aircraft measurements, Atmos. Chem. Phys., 9, 1723-1734,

doi:10.5194/acp-9-1723-2009, 2009.

Collier, A. B., and Hughes, A. R.: Lightning and the African ITCZ, J. Atmos. Sol-Terr. Phy., 73, 2392-2398,

doi:10.1016/j.jastp.2011.08.010, 2011.

580     Cooper, O., Moody, J., Parrish, D., Trainer, M., Ryerson, T., Holloway, J., Hübler, G., Fehsenfeld, F., and Evans, M.: Trace

gas composition of midlatitude cyclones over the western North Atlantic Ocean: A conceptual model, J. Geophys. Res.,

107, 5-24, doi:10.1029/2001jd000901, 2002.

Cooper, O., Parrish, D., Stohl, A., Trainer, M., Nédélec, P., Thouret, V., Cammas, J.-P., Oltmans, S., Johnson, B., and Tarasick, D.: Increasing springtime ozone mixing ratios in the free troposphere over western North America, Nature, 463, 344-348, doi:10.1038/nature08708, 2010.

Cooper, O., Oltmans, S., Johnson, B., Brioude, J., Angevine, W., Trainer, M., Parrish, D., Ryerson, T., Pollack, I., and Cullis, P.: Measurement of western US baseline ozone from the surface to the tropopause and assessment of downwind impact regions, J. Geophys. Res., 116, 898-908, doi:10.1029/2011JD016095, 2011.

Cooper, O. R., Langford, A. O., Parrish, D. D., and Fahey, D. W.: Challenges of a lowered US ozone standard, Science, 348, 1096-1097, doi:10.1126/science.aaa5748, 2015.

Derwent, R. G., Utembe, S. R., Jenkin, M. E., and Shallcross, D. E.: Tropospheric ozone production regions and the intercontinental origins of surface ozone over Europe, Atmos. Environ., 112, 216-224, doi:10.1016/j.atmosenv.2015.04.049, 2015.

Derwent, R. G., Parrish, D. D., Galbally, I. E., Stevenson, D. S., Doherty, R. M., Young, P. J., and Shallcross, D. E.: Interhemispheric differences in seasonal cycles of tropospheric ozone in the marine boundary layer: Observation-model comparisons, J. Geophys. Res., 121, 11075-11085, doi:10.1002/2016JD024836, 2016.

Diedhiou, A., Janicot, S., Viltard, A., De Felice, P., and Laurent, H.: Easterly wave regimes and associated convection over West Africa and tropical Atlantic: results from the NCEP/NCAR and ECMWF reanalyses, Clim. Dynam., 15, 795-822, 10.1007/s003820050316, 1999.

Ding, Y., and Chan, J. C. L.: The East Asian summer monsoon: an overview, Meteorol. Atmos. Phys., 89, 117-142, doi:10.1007/s00703-005-0125-z, 2005.

Ding, Y. Liu, Y. Song, Y., and Zhang, J.: From MONEX to the Global Monsoon: A Review of Monsoon System Research, Adv. Atmos. Sci., 32, 10-31, doi:10.1007/s00376-014-0008-7, 2015.

Doherty, O. M., Riemer, N., and Hameed, S.: Control of Saharan mineral dust transport to Barbados in winter by the Intertropical Convergence Zone over West Africa, J. Geophys. Res., 117, 161-169, doi:10.1029/2012JD017767, 2012.

Doherty, O. M., Riemer, N., and Hameed, S.: Role of the convergence zone over West Africa in controlling Saharan mineral

dust load and transport in the boreal summer, Tellus B, 66, 759-763, doi:10.3402/tellusb.v66.23191, 2014.

Doherty, R., Wild, O., Shindell, D., Zeng, G., MacKenzie, I., Collins, W., Fiore, A. M., Stevenson, D., Dentener, F., and Schultz, M.: Impacts of climate change on surface ozone and intercontinental ozone pollution: A multi-model study, J.

610     Geophys. Res., 118, 3744-3763, doi:10.1002/jgrd.50266, 2013.

Doherty, R. M.: Atmospheric chemistry: Ozone pollution from near and far, Nat. Geosci., 8, 664-665, doi:10.1038/ngeo2497, 2015.

Draxler, R. R., and Hess, G.: An overview of the HYSPLIT_4 modelling system for trajectories, Aust. Meteorol. Mag., 47, 295-308, 1998.

615     Duncan, B. N., Martin, R. V., Staudt, A. C., Yevich, R., and Logan, J. A.: Interannual and seasonal variability of biomass burning emissions constrained by satellite observations, J. Geophys. Res., 108, ACH 1-1-ACH 1-22, doi:10.1029/2002JD002378, 2003.

Fiore, A. M., Jacob, D. J., Bey, I., Yantosca, R. M., Field, B. D., Fusco, A. C., and Wilkinson, J. G.: Background ozone over the United States in summer: Origin, trend, and contribution to pollution episodes, J. Geophys. Res., 107, ACH 11-1-ACH

620     11-25, doi:10.1029/2001JD000982, 2002.

Fiore, A. M., Dentener, F., Wild, O., Cuvelier, C., Schultz, M., Hess, P., Textor, C., Schulz, M., Doherty, R., and Horowitz, L.: Multimodel estimates of intercontinental source-receptor relationships for ozone pollution, J. Geophys. Res., 114, 83-84, doi:10.1029/2008JD010816, 2009.

Fleming, Z. L., Monks, P. S., and Manning, A. J.: Review: Untangling the influence of air-mass history in interpreting

625     observed atmospheric composition, Atmos. Res., 104, 1-39, doi:10.1016/j.atmosres.2011.09.009, 2012.

Fukutomi, Y., and Yasunari, T.: Structure and characteristics of submonthly-scale waves along the Indian Ocean ITCZ, Clim. Dynam., 40, 1819-1839, doi:10.1007/s00382-012-1417-x, 2013.

Fukutomi, Y., and Yasunari, T.: Extratropical forcing of tropical wave disturbances along the Indian Ocean ITCZ, J. Geophys. Res., 119, 1154-1171, doi:10.1002/2013JD020696, 2014.

630     Garny, H., and Randel, W. J.: Transport pathways from the Asian monsoon anticyclone to the stratosphere, Atmos. Chem.

Phys., 16, 2703-2718, doi:10.5194/acp-16-2703-2016, 2016.

Giglio, L., Randerson, J. T., and Werf, G. R.: Analysis of daily, monthly, and annual burned area using the fourth-generation global fire emissions database (GFED4), J. Geophys. Res., 118, 317-328, doi:10.1002/jgrg.20042, 2013.

Guenther, A., Jiang, X., Heald, C., Sakulyanontvittaya, T., Duhl, T., Emmons, L., and Wang, X.: The Model of Emissions of Gases and Aerosols from Nature version 2.1 (MEGAN2.1): an extended and updated framework for modeling biogenic emissions, Geosci. Model Dev., 5, 1471-1492, doi:10.5194/gmd-5-1471-2012, 2012.

Guerova, G., Bey, I., Attié, J.-L., Martin, R., Cui, J., and Sprenger, M.: Impact of transatlantic transport episodes on summertime ozone in Europe, Atmos. Chem. Phys., 6, 2057-2072, doi:10.5194/acp-6-2057-2006, 2006.

Hack, J. J.: Parameterization of moist convection in the National Center for Atmospheric Research community climate model (CCM2), J. Geophys. Res., 99, 5551-5568, doi:10.1029/93jd03478, 1994.

Halpern, D., and Woiceshyn, P. M.: Onset of the Somali Jet in the Arabian Sea during June 1997, J. Geophys. Res., 104, 18041-18046, doi:10.1029/1999jc900141, 1999.

Halpern, D., and Woiceshyn, P. M.: Somali Jet in the Arabian Sea, El Niño, and India Rainfall, J. Climate, 14, 434-441, doi:10.1175/1520-0442(2001)014<0434:sjitas>2.0.co;2, 2001.

Hartley, D. E., and Black, R. X.: Mechanistic analysis of interhemispheric transport, Geophys. Res. Lett., 22, 2945-2948, doi:10.1029/95gl02823, 1995.

Hollaway, M. J., Arnold, S., Challinor, A. J., and Emberson, L.: Intercontinental trans-boundary contributions to ozone-induced crop yield losses in the Northern Hemisphere, Biogeosciences, 9, 271-292, doi:10.5194/bg-9-271-2012, 2012.

Holloway, T., Sakurai, T., Han, Z., Ehlers, S., Spak, S. N., Horowitz, L. W., Carmichael, G. R., Streets, D. G., Hozumi, Y., and Ueda, H.: MICS-Asia II: Impact of global emissions on regional air quality in Asia, Atmos. Environ., 42, 3543-3561, doi:10.1016/j.atmosenv.2007.10.022, 2008.

HTAP: Hemispheric transport of air pollution 2010, United Nations, Dentener, F., Keating, T. and Akimoto, H. (eds.), New York and Geneva, 2010.

Hu, Y., Li, D., and Liu, J.: Abrupt seasonal variation of the ITCZ and the Hadley circulation, Geophys. Res. Lett., 34, 5407-

655        5413, doi:10.1029/2007GL030950, 2007.

Huang, R., Chen, J., Wang, L., and Lin, Z.: Characteristics, processes, and causes of the spatio-temporal variabilities of the

East Asian monsoon system, Adv. Atmos. Sci., 29, 910-942, doi: 10.1007/s00376-012-2015-x, 2012.

Huang, M., Carmichael, G. R., Pierce, R. B., Jo, D. S., Park, R. J., Flemming, J., Emmons, L. K., Bowman, K. W., Henze, D.

K., Davila, Y., Sudo, K., Jonson, J. E., Tronstad Lund, M., Janssens-Maenhout, G., Dentener, F. J., Keating, T. J., Oetjen,

660        H., and Payne, V. H.: Impact of intercontinental pollution transport on North American ozone air pollution: an HTAP

phase 2 multi-model study, Atmos. Chem. Phys., 17, 5721-5750, doi:10.5194/acp-17-5721-2017, 2017.

Huntrieser, H., Heland, J., Schlager, H., Forster, C., Stohl, A., Aufmhoff, H., Arnold, F., Scheel, H., Campana, M., and Gilge,

S.: Intercontinental air pollution transport from North America to Europe: Experimental evidence from airborne

measurements and surface observations, J. Geophys. Res., 110, 372-384, doi:10.1029/2004JD005045, 2005.

665    Ikeda, K., Tanimoto, H., Sugita, T., Akiyoshi, H., Kanaya, Y., Zhu, C., and Taketani, F.: Tagged tracer simulations of black

carbon in the Arctic: transport, source contributions, and budget, Atmos. Chem. Phys., 17, 10515-10533, doi:10.5194/acp-

17-10515-2017, 2017.

Jaffe, D., McKendry, I., Anderson, T., and Price, H.: Six 'new' episodes of trans-Pacific transport of air pollutants, Atmos.

Environ., 37, 391-404, doi:10.1016/s1352-2310(02)00862-2, 2003.

670    Jiang, Z., Miyazaki, K., Worden, J. R., Liu, J. J., Jones, D. B. A., and Henze, D. K.: Impacts of anthropogenic and natural

sources on free tropospheric ozone over the Middle East, Atmos. Chem. Phys., 16, 6537-6546, doi:10.5194/acp-16-6537-

2016, 2016.

Jones, C., Mahowald, N., and Luo, C.: The role of easterly waves on African desert dust transport, J. Climate, 16, 3617-3628,

doi:10.1175/1520-0442(2003)016<3617:troewo>2.0.co;2, 2003.

675    Joseph, P., and Sijikumar, S.: Intraseasonal variability of the low-level jet stream of the Asian summer monsoon, J. Climate,

17, 1449-1458, doi:10.1175/1520-0442(2004)017<1449:ivotlj>2.0.co;2, 2004.

Kalnay, E., Kanamitsu, M., Kistler, R., Collins, W., Deaven, D., Gandin, L., Iredell, M., Saha, S., White, G., and Woollen, J.:

The NCEP/NCAR 40-year reanalysis project, Bull. Amer. Meteor. Soc., 77, 437-471, doi:10.1175/1520-

0477(1996)077<0437:tnyrp>2.0.co;2, 1996.

680 Kim, M. J., Park, R. J., Ho, C.-H., Woo, J.-H., Choi, K.-C., Song, C.-K., and Lee, J.-B.: Future ozone and oxidants change under the RCP scenarios, Atmos. Environ., 101, 103-115, doi:10.1016/j.atmosenv.2014.11.016, 2015.

Koumoutsaris, S., Bey, I., Generoso, S., and Thouret, V.: Influence of El Niño-Southern Oscillation on the interannual variability of tropospheric ozone in the northern midlatitudes, J. Geophys. Res., 113, D19301, doi:10.1029/2007JD009753, 2008.

685 Kuhns, H., Green, M., and Etyemezian, V.: Big Bend Regional Aerosol and Visibility Observational (BRAVO) Study Emissions Inventory, 2003.

Lacis, A. A., Wuebbles, D. J., and Logan, J. A.: Radiative forcing of climate by changes in the vertical distribution of ozone, J. Geophys. Res., 95, 9971-9981, doi:10.1029/jd095id07p09971, 1990.

Lal, S., Venkataramani, S., Chandra, N., Cooper, O. R., Brioude, J., and Naja, M.: Transport effects on the vertical

690 distribution of tropospheric ozone over western India, J. Geophys. Res., 119, 10012-10026, doi:10.1002/2014JD021854, 2014.

Lefohn, A. S., Malley, C. S., Simon, H., Wells, B., Xu, X., Zhang, L., and Wang, T.: Responses of human health and vegetation exposure metrics to changes in ozone concentration distributions in the European Union, United States, and China, Atmos. Environ., 152, 123-145, doi:10.1016/j.atmosenv.2016.12.025, 2017.

695 Lelieveld, J., and Dentener, F. J.: What controls tropospheric ozone?, J. Geophys. Res., 105, 3531-3551, doi:10.1029/1999jd901011, 2000.

Lewis, A., Evans, M., Methven, J., Watson, N., Lee, J., Hopkins, J., Purvis, R., Arnold, S., McQuaid, J., and Whalley, L.: Chemical composition observed over the mid-Atlantic and the detection of pollution signatures far from source regions, J. Geophys. Res., 112, 815-838, doi:10.1029/2006JD007584, 2007.

700 Li, X., Liu, J., Mauzerall, D. L., Emmons, L. K., Walters, S., Horowitz, L. W., and Tao, S.: Effects of trans-Eurasian transport of air pollutants on surface ozone concentrations over Western China, J. Geophys. Res., 119, 12338-12354, doi:10.1002/2014jd021936, 2014.

Li, Z., Lau, W. K. M., Ramanathan, V., Wu, G., Ding, Y., Manoj, M. G., Liu, J., Qian, Y., Li, J., and Zhou, T.: Aerosol and monsoon climate interactions over Asia, Rev. Geophys., 54, 866–929, doi:10.1002/2015RG000500, 2016.

705 Liebmann, B., and Smith, C. A.: Description of a complete (interpolated) outgoing longwave radiation dataset, Bull. Amer. Meteor. Soc., 77, 1275-1277, 1996.

Lin, M., Horowitz, L. W., Payton, R., Fiore, A. M., and Tonnesen, G.: US surface ozone trends and extremes from 1980 to 2014: quantifying the roles of rising Asian emissions, domestic controls, wildfires, and climate, Atmos. Chem. Phys., 17, 2943-2970, doi:10.5194/acp-17-2943-2017, 2017.

710 Liu, H., Jacob, D. J., Chan, L. Y., Oltmans, S. J., Bey, I., Yantosca, R. M., Harris, J. M., Duncan, B. N., and Martin, R. V.: Sources of tropospheric ozone along the Asian Pacific Rim: An analysis of ozonesonde observations, J. Geophys. Res., 107, ACH 3-1-ACH 3-19, doi:10.1029/2001JD002005, 2002.

Liu, J. J., Jones, D., Worden, J. R., Noone, D., Parrington, M., and Kar, J.: Analysis of the summertime buildup of tropospheric ozone abundances over the Middle East and North Africa as observed by the Tropospheric Emission 715 Spectrometer instrument, J. Geophys. Res., 114, 730-734, doi:10.1029/2008JD010993, 2009.

Liu, J. J., Jones, D., Zhang, S., and Kar, J.: Influence of interannual variations in transport on summertime abundances of ozone over the Middle East, J. Geophys. Res., 116, 999-1010, doi:10.1029/2011JD016188, 2011.

Long, M., Yantosca, R., Nielsen, J., Keller, C., da Silva, A., Sulprizio, M., Pawson, S., and Jacob, D.: Development of a grid-independent GEOS-Chem chemical transport model (v9-02) as an atmospheric chemistry module for Earth system models, 720 Geosci. Model. Dev., 8, 595-602, doi:10.5194/gmd-8-595-2015, 2015.

Marais, E. A., Jacob, D. J., Kurosu, T. P., Chance, K., Murphy, J. G., Reeves, C., Mills, G., Casadio, S., Millet, D. B., Barkley, M. P., Paulot, F., and Mao, J.: Isoprene emissions in Africa inferred from OMI observations of formaldehyde columns, Atmos. Chem. Phys., 12, 6219-6235, doi:10.5194/acp-12-6219-2012, 2012.

Mari, C., Cailley, G., Corre, L., Saunois, M., Attié, J., Thouret, V., and Stohl, A.: Tracing biomass burning plumes from the 725 Southern Hemisphere during the AMMA 2006 wet season experiment, Atmos. Chem. Phys., 8, 3951-3961, doi:10.5194/acp-8-3951-2008, 2008.

Miyazaki, K., Eskes, H., Sudo, K., and Zhang, C.: Global lightning NO x production estimated by an assimilation of multiple satellite data sets, Atmos. Chem. Phys., 14, 3277-3305, doi:10.5194/acp-14-3277-2014, 2014.

Monks, P. S., Archibald, A., Colette, A., Cooper, O., Coyle, M., Derwent, R., Fowler, D., Granier, C., Law, K. S., and Mills, G.: Tropospheric ozone and its precursors from the urban to the global scale from air quality to short-lived climate forcer, Atmos. Chem. Phys., 15, 8889-8973, doi:10.5194/acp-15-8889-2015, 2015.

Mounier, F., and Janicot, S.: Evidence of two independent modes of convection at intraseasonal timescale in the West African summer monsoon, Geophys. Res. Lett., 31, 2876-2877, doi:10.1029/2004GL020665, 2004.

Myhre, G., Shindell, D., Bréon, F.-M., Collins, W., Fuglestvedt, J., Huang, J., Koch, D., Lamarque, J.-F., Lee, D., Mendoza, B., Nakajima, T., Robock, A., Stephens, G., Takemura, T., and Zhang, H.: Anthropogenic and Natural Radiative Forcing, In: Climate Change 2013: The Physical Science Basis, Contribution of Working Group I to the Fifth Assessment Report of the Intergovernmental Panel on Climate Change, Cambridge University Press, Cambridge, United Kingdom and New York, NY, USA, 659-740, 2013.

Nagashima, T., Ohara, T., Sudo, K., and Akimoto, H.: The relative importance of various source regions on East Asian surface ozone, Atmos. Chem. Phys., 10, 11305-11322, doi:10.5194/acp-10-11305-2010, 2010.

Neu, J. L., Flury, T., Manney, G. L., Santee, M. L., Livesey, N. J., and Worden, J.: Tropospheric ozone variations governed by changes in stratospheric circulation, Nat. Geosci., 7, 340-344, doi:10.1038/NGEO2138, 2014.

Nicholson, S. E., and Grist, J. P.: The seasonal evolution of the atmospheric circulation over West Africa and equatorial Africa, J. Climate, 16, 1013-1030, doi:10.1175/1520-0442(2003)016<1013:tseota>2.0.co;2, 2003.

Nicholson, S. E.: The intensity, location and structure of the tropical rainbelt over west Africa as factors in interannual variability, Int. J.Climatol., 28, 1775-1785, doi:10.1002/joc.1507, 2008.

Nicholson, S. E.: A revised picture of the structure of the "monsoon" and land ITCZ over West Africa, Clim. Dynam., 32, 1155-1171, doi:10.1007/s00382-008-0514-3, 2009.

Nützel, M., Dameris, M., and Garny, H.: Movement, drivers and bimodality of the South Asian High, Atmos. Chem. Phys., 16, 14755-14774, doi:10.5194/acp-16-14755-2016, 2016.

Olivier, J.G.J. and J.J.M. Berdowski, Global emissions sources and sinks. In: Berdowski, J., Guicherit, R. and B.J. Heij (eds.) The Climate System, pp. 33-78. A. A. Balkema Publishers/Swets & Zeitlinger Publishers, Lisse, The Netherlands., 2001

Ott, L. E., Pickering, K. E., Stenchikov, G. L., Allen, D. J., Decaria, A. J., Ridley, B., Lin, R. F., Lang, S., and Tao, W. K.: Production of lightning NOx and its vertical distribution calculated from three-dimensional cloud-scale chemical transport model simulations, J. Geophys. Res., 115, 288-303, doi:10.1029/2009JD011880, 2010.

Philip, S., Martin, R. V., and Keller, C. A.: Sensitivity of chemistry-transport model simulations to the duration of chemical and transport operators: a case study with GEOS-Chem v10-01, Geosci. Model. Dev., 9, 1683-1695, doi:10.5194/gmd-9-1683-2016, 2016.

Pickering, K. E., Wang, Y., Tao, W. K., Price, C., and Müller, J. F.: Vertical distributions of lightning NOx for use in regional and global chemical transport models, J. Geophys. Res., 103, 31203-31216, doi:10.1029/98jd02651, 1998.

Piketh, S. J. and Walton, N. W.: Characteristics of Atmospheric Transport of Air Pollution for Africa, In: Stohl, A., ed., Intercontinental Transport of Air Pollution, Springer Berlin Heidelberg, 173-197, 2004.

Pochanart, P., Akimoto, H., Kajii, Y., and Sukasem, P.: Carbon monoxide, regional‐scale transport, and biomass burning in tropical continental Southeast Asia: Observations in rural Thailand, J. Geophys. Res., 108, 1337-1352, doi:doi:10.1029/2002JD003360, 2003.

Pochanart, P., Wild, O., and Akimoto, H.: Air pollution import to and export from East Asia, Air Pollution, 99-130, 2004.

Pulles, T., Bolscher, M. V. H., Brand, R., and Visschedijk, A.: Assessment of Global Emissions from Fuel Combustion in the Final Decades of the 20th Century, TNO report A-R0132/B, 2007.

Raper, J. L., Kleb, M. M., Jacob, D. J., Davis, D. D., Newell, R. E., Fuelberg, H. E., Bendura, R. J., Hoell, J. M., and McNeal, R. J.: Pacific Exploratory Mission in the Tropical Pacific- PEM-Tropics B, March-April 1999, J. Geophys. Res., 106, 32401-32425, doi:10.1029/2000JD900833, 2001.

Rastigejev, Y., Park, R., Brenner, M. P., and Jacob, D. J.: Resolving intercontinental pollution plumes in global models of atmospheric transport, J. Geophys. Res., 115, D02302, doi:10.1029/2009JD012568, 2010.

Ridder, T., Gerbig, C., Notholt, J., Rex, M., Schrems, O., Warneke, T., and Zhang, L.: Ship-borne FTIR measurements of CO

and O$_3$ in the Western Pacific from 43°N to 35°S: an evaluation of the sources, Atmos. Chem. Phys., 12, 815-828, doi:10.5194/acp-12-815-2012, 2012.

Rodríguez, S., Cuevas, E., Prospero, J., Alastuey, A., Querol, X., López-Solano, J., García, M., and Alonso-Pérez, S.: Modulation of Saharan dust export by the North African dipole, Atmos. Chem. Phys., 15, 7471-7486, doi:10.5194/acp-15-7471-2015, 2015.

Sauvage, B., Thouret, V., Cammas, J.-P., Gheusi, F., Athier, G., and Nédélec, P.: Tropospheric ozone over Equatorial Africa: regional aspects from the MOZAIC data, Atmos. Chem. Phys., 5, 311-335, doi:10.5194/acp-5-311-2005, 2005.

Sekiya, T., and Sudo, K.: Role of meteorological variability in global tropospheric ozone during 1970-2008, J. Geophys. Res., 117, D18303, doi:10.1029/2012JD018054, 2012.

Sekiya, T., and Sudo, K.: Roles of transport and chemistry processes in global ozone change on interannual and multidecadal time scales, J. Geophys. Res., 119, 4903-4921, doi:10.1002/2013JD020838, 2014.

Stein, A. F., Draxler, R. R., Rolph, G. D., Stunder, B. J. B., Cohen, M. D., and Ngan, F.: NOAA's HYSPLIT Atmospheric Transport and Dispersion Modeling System, Bull. Amer. Meteor. Soc., 96, 2059-2077, doi:10.1175/bams-d-14-00110.1, 2015.

Streets, D. G., Bond, T. C., Carmichael, G. R., Fernandes, S. D., He, D., Klimont, Z., Nelson, S. M., Tsai, N. Y., and Wang, M. Q.: An inventory of gaseous and primary aerosol emissions in Asia in the year 2000, J. Geophys. Res., 108, GTE 30-1-GTE 30-23, doi:10.1029/2002JD003093, 2003.

Streets, D. G., Zhang, Q., Wang, L., He, K., Hao, J., Wu, Y., Tang, Y., and Carmichael, G. R.: Revisiting China's CO emissions after the Transport and Chemical Evolution over the Pacific (TRACE-P) mission: Synthesis of inventories, atmospheric modeling, and observations, J. Geophys. Res., 111, D14306, doi:10.1029/2006JD007118, 2006.

Sudo, K., and Akimoto, H.: Global source attribution of tropospheric ozone: Long-range transport from various source regions, J. Geophys. Res., 112, D12302, doi:10.1029/2006JD007992, 2007.

Sultan, B., and Janicot, S.: Abrupt shift of the ITCZ over West Africa and intra-seasonal variability, Geophys. Res. Lett., 27, 3353-3356, doi:10.1029/1999gl011285, 2000.

Suzuki, T.: Seasonal variation of the ITCZ and its characteristics over central Africa, Theor. Appl. Climatol., 103, 39-60,

800      doi:10.1007/s00704-010-0276-9, 2011.

Thompson, A. M.: Intercontinental Transport of Ozone from Tropical Biomass Burning, In: Stohl, A., ed., Intercontinental

Transport of Air Pollution, Springer Berlin Heidelberg, 225-254, 2004.

Thompson, A. M., Miller, S. K., Tilmes, S., Kollonige, D. W., Witte, J. C., Oltmans, S. J., Johnson, B. J., Fujiwara, M.,

Schmidlin, F., and Coetzee, G.: Southern Hemisphere Additional Ozonesondes (SHADOZ) ozone climatology (2005-

805      2009): Tropospheric and tropical tropopause layer (TTL) profiles with comparisons to OMI-based ozone products, J.

Geophys. Res., 117, D23301, doi:10.1029/2011JD016911, 2012.

Thompson, A. M., Balashov, N. V., Witte, J., Coetzee, J., Thouret, V., and Posny, F.: Tropospheric ozone increases over the

southern Africa region: bellwether for rapid growth in Southern Hemisphere pollution?, Atmos. Chem. Phys., 14, 9855-

9869, doi:10.5194/acp-14-9855-2014, 2014.

810    Tie, X., Guenther, A., and Holland, E.: Biogenic methanol and its impacts on tropospheric oxidants, Geophys. Res. Lett., 30,

ASC 3-1-ASC 3-3, doi:10.1029/2003GL017167, 2003.

Van der Werf, G. R., Randerson, J. T., Giglio, L., Collatz, G. J., Mu, M., Kasibhatla, P. S., Morton, D. C., Defries, R. S., Jin,

Y., and Leeuwen, T. T. V.: Global fire emissions and the contribution of deforestation, savanna, forest, agricultural, and

peat fires (1997–2009), Atmos. Chem. Phys., 10, 16153-16230, doi:10.5194/acp-10-11707-2010, 2010.

815    Verstraeten, W. W., Neu, J. L., Williams, J. E., Bowman, K. W., Worden, J. R., and Boersma, K. F.: Rapid increases in

tropospheric ozone production and export from China, Nat. Geosci., 8, 690-695, doi:10.1038/NGEO2493, 2015.

Vestreng, V., and Klein, H.: Emission data reported to UNECE/EMEP: Quality assurance and trend analysis & Presentation

of WebDab, MSC-W Status Report 2002, Norwegian Meteorological Institute, Oslo Norway, July 2002.

Vogel, B., Günther, G., Müller, R., Grooß, J.-U., Hoor, P., Krämer, M., Müller, S., Zahn, A., and Riese, M.: Fast transport

820    from Southeast Asia boundary layer sources to northern Europe: rapid uplift in typhoons and eastward eddy shedding of

the Asian monsoon anticyclone, Atmos. Chem. Phys., 14, 12745-12762, doi:10.5194/acp-14-12745-2014, 2014.

Waliser, D. E., and Gautier, C.: A satellite-derived climatology of the ITCZ, J. Climate, 6, 2162-2174, doi:10.1175/1520-

0442(1993)006<2162:asdcot>2.0.co;2, 1993.

Waliser, D. E., Graham, N. E., and Gautier, C.: Comparison of the highly reflective cloud and outgoing longwave radiation

825     datasets for use in estimating tropical deep convection, J. Climate, 6, 331-353, doi:10.1175/1520-
0442(1993)006<0331:cothrc>2.0.co;2, 1993.

Wang, Y., Logan, J. A., and Jacob, D. J.: Global simulation of tropospheric $O_3$-$NO_x$-hydrocarbon chemistry: 2. Model
evaluation and global ozone budget, J. Geophys. Res., 103, 10727-10755, doi:10.1029/98jd00157, 1998.

Wang, Y., Zhang, Y., Hao, J., and Luo, M.: Seasonal and spatial variability of surface ozone over China: contributions from

830     background and domestic pollution, Atmos. Chem. Phys., 11, 3511-3525, doi:10.5194/acp-11-3511-2011, 2011.

Wild, O., Law, K. S., McKenna, D. S., Bandy, B. J., Penkett, S. A., and Pyle, J. A.: Photochemical trajectory modeling
studies of the North Atlantic region during August 1993, J. Geophys. Res., 101, 29269-29288, doi:10.1029/96jd00837,
1996.

Wild, O., Pochanart, P., and Akimoto, H.: Trans-Eurasian transport of ozone and its precursors, J. Geophys. Res., 109,

835     D11302, doi:10.1029/2003JD004501, 2004.

Williams, J., Scheele, M., Van Velthoven, P., Cammas, J.-P., Thouret, V., Galy-Lacaux, C., and Volz-Thomas, A.: The
influence of biogenic emissions from Africa on tropical tropospheric ozone during 2006: a global modeling study, Atmos.
Chem. Phys., 9, 5729-5749, doi:10.5194/acp-9-5729-2009, 2009.

Wu, G., Liu, Y., Bian, H., Bao, Q., Duan, A., and Jin, F. F.: Thermal Controls on the Asian Summer Monsoon, Sci. Rep., 2,

840     404, doi:10.1038/srep00404, 2012.

Wu, G., Duan, A., Liu, Y., Mao, J., Ren, R., Bao, Q., He, B., Liu, B., and Hu, W.: Tibetan Plateau climate dynamics: recent
research progress and outlook, Natl. Sci. Rev., 2, 100-116, doi:10.1093/nsr/nwu045, 2015.

Xie, S.-P.: The shape of continents, air-sea interaction, and the rising branch of the Hadley circulation, in: The Hadley
Circulation: Present, Past and Future, Springer, 121-152, 2004.

845     Yevich, R., and Logan, J. A.: An assessment of biofuel use and burning of agricultural waste in the developing world, Global
Biogeochem. Cy., 17, 1095, doi:10.1029/2002GB001952, 2003.

Žagar, N., Skok, G., and Tribbia, J.: Climatology of the ITCZ derived from ERA Interim reanalyses, J. Geophys. Res., 116, D15103, doi:10.1029/2011JD015695, 2011.

Zare, A., Christensen, J. H., Gross, A., Irannejad, P., Glasius, M., and Brandt, J.: Quantifying the contributions of natural emissions to ozone and total fine PM concentrations in the Northern Hemisphere, Atmos. Chem. Phys., 14, 2735-2756, doi:10.5194/acp-14-2735-2014, 2014.

Zhang, G. J., and McFarlane, N. A.: Sensitivity of climate simulations to the parameterization of cumulus convection in the Canadian climate centre general circulation model, Atmos. Ocean., 33, 407-446, doi:10.1080/07055900.1995.9649539, 1995.

Zhang, Y., Li, T., Wang, B., and Wu, G.: Onset of the Summer Monsoon over the Indochina Peninsula: Climatology and Interannual Variations, J. Climate, 15, 3206-3221, doi:10.1175/1520-0442(2002)015<3206:ootsmo>2.0.co;2, 2002.

Zhang, L., Jacob, D. J., Boersma, K. F., Jaffe, D. A., Olson, J. R., Bowman, K. W., Worden, J. R., Thompson, A. M., Avery, M. A., Cohen, R. C., Dibb, J. E., Flock, F. M., Fuelberg, H. E., Huey, L. G., McMillan, W. W., Singh, H. B., and Weinheimer, A. J.: Transpacific transport of ozone pollution and the effect of recent Asian emission increases on air quality in North America: an integrated analysis using satellite, aircraft, ozonesonde, and surface observations, Atmos. Chem. Phys., 8, 6117-6136, doi:10.5194/acp-8-6117-2008, 2008.

Zhao, T., Gong, S., Zhang, X., and McKendry, I.: Modeled size-segregated wet and dry deposition budgets of soil dust aerosol during ACE-Asia 2001: Implications for trans-Pacific transport, J. Geophys. Res., 108, 420-424, doi:10.1029/2002JD003363, 2003.

Zhao, T., Gong, S., Huang, P., and Lavoué, D.: Hemispheric transport and influence of meteorology on global aerosol climatology, Atmos. Chem. Phys., 12, 7609-7624, doi:10.5194/acp-12-7609-2012, 2012.

Zhu, Y.: Variations of the summer Somali and Australia cross-equatorial flows and the implications for the Asian summer monsoon, Adv. Atmos. Sci., 29(3), 509-518, doi:10.1007/s00376-011-1120-6, 2012.

Zhu, B., Hou, X., and Kang, H.: Analysis of the seasonal ozone budget and the impact of the summer monsoon on the northeastern Qinghai-Tibetan Plateau, J. Geophys. Res., 121, 2029-2042, doi:10.1002/2015JD023857, 2016.

Zhu, J., Liao, H., Mao, Y., Yang, Y., and Jiang, H.: Interannual variation, decadal trend, and future change in ozone outflow from East Asia, Atmos. Chem. Phys., 17, 3729-3747, doi:10.5194/acp-17-3729-2017, 2017a.

Zhu, Y., Liu, J., Wang, T., Zhuang, B., Han, H., Wang, H., Chang, Y., and Ding, K.: The impacts of meteorology on the seasonal and interannual variabilities of ozone transport from North America to East Asia, J. Geophys. Res., 122, doi:10.1002/2017JD026761, 2017b.

875
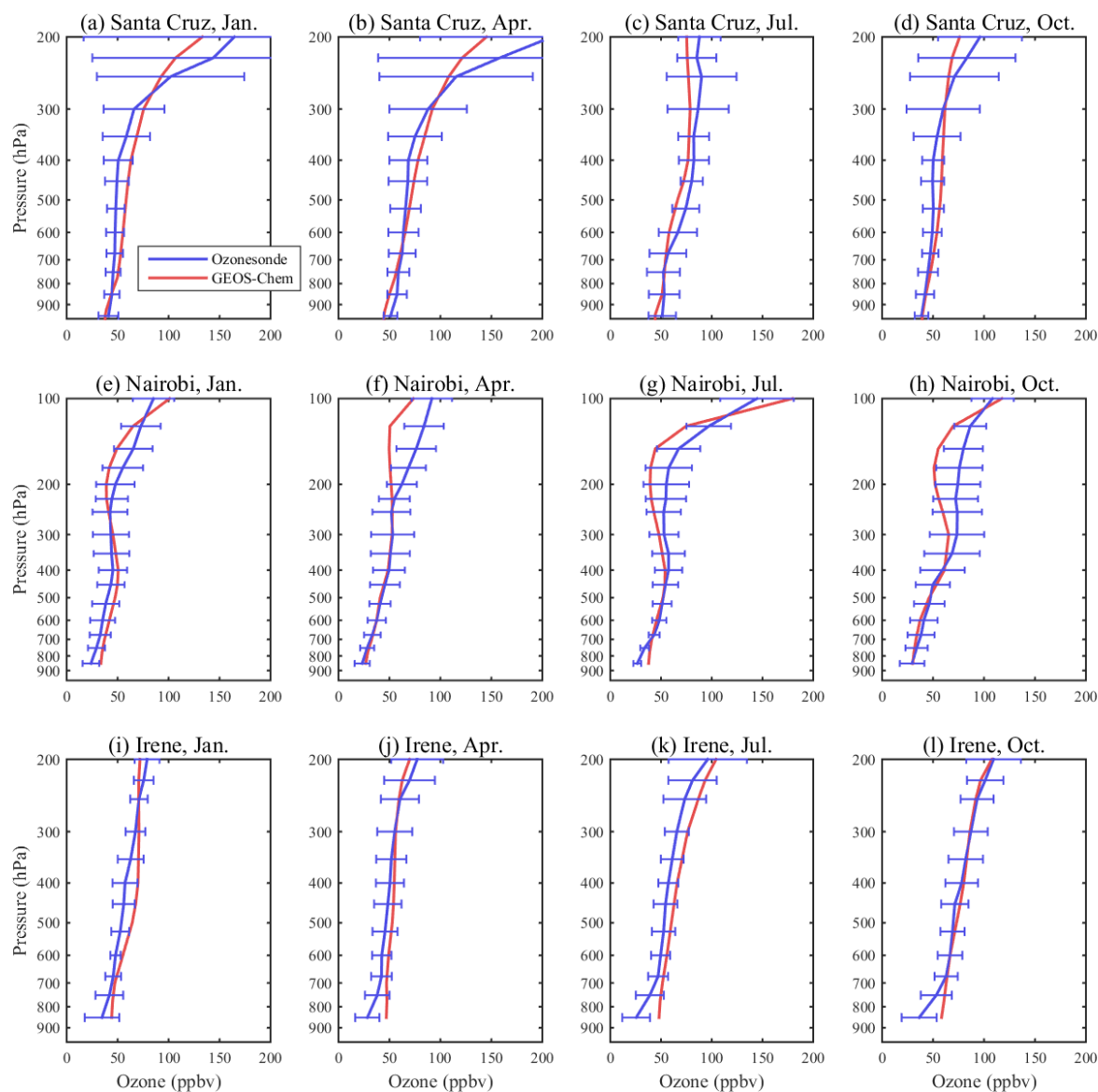
Figure 1. Comparison of the monthly mean ozone vertical profiles between the GEOS-Chem simulations (read line) and the ozonesonde measurements (blue line) at Santa Cruz (1st row), Nairobi (2nd row), and Irene (3rd row) in Africa, in January (1st col.), April (2nd col.), July (3rd col.), and October (4th col.), respectively. The horizontal bar indicates the standard deviation.
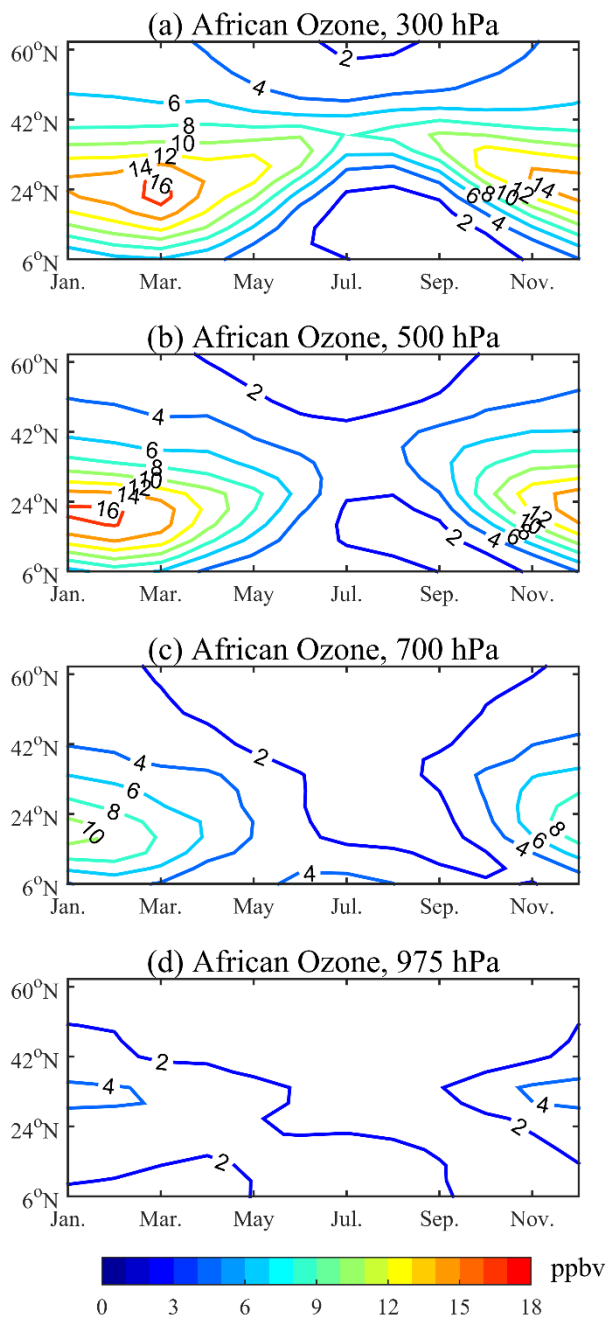
Figure 2. Seasonal variation of imported African ozone (in ppbv) over Asia varying with latitude at (a)

300 hPa, (b) 500 hPa, (c) 700 hPa, and (d) 975 hPa. The values are the 20-year means (1987-2006) from

the GEOS-Chem simulation and averaged over 60-145°E.
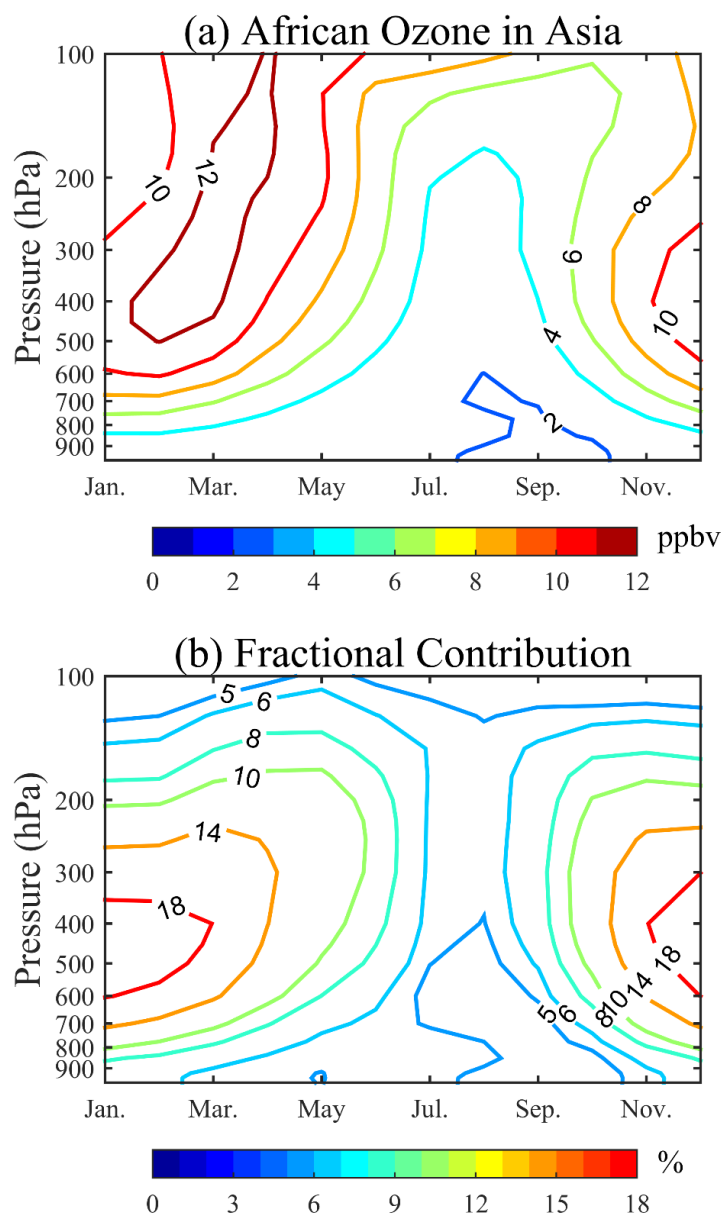
Figure 3. (a) Seasonal variation of imported African ozone (in ppbv) varying with altitude. (b) The same as (a) but for the corresponding fractional contribution (in %). The values are the 20-year means (1987-2006) from the GEOS-Chem simulation and averaged over Asia (60-145°E, 5-40°N).
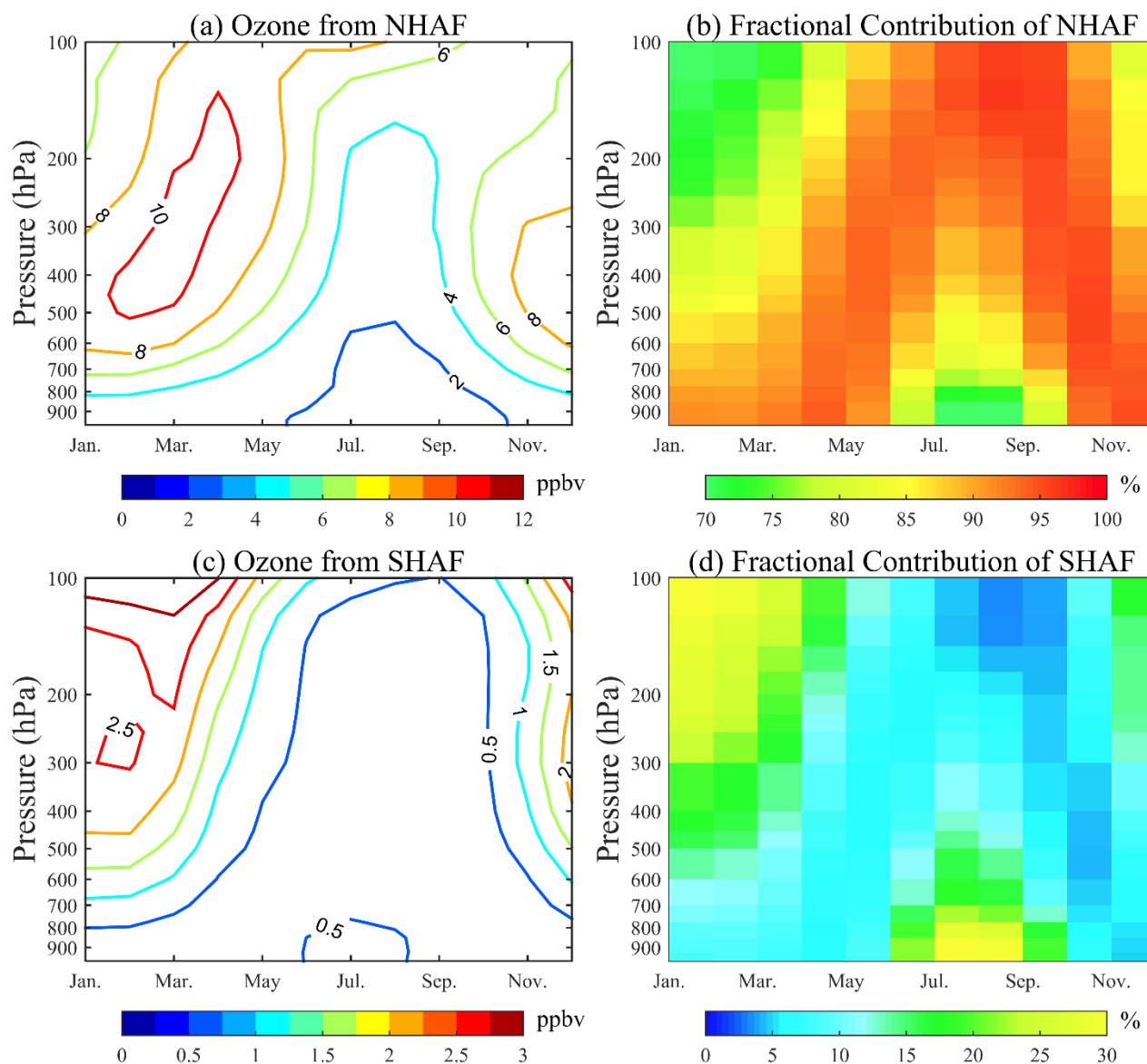
Figure 4. Seasonal-altitude variations of imported ozone (in ppbv) from (a) NHAF and (c) SHAF over Asia (60-145°E, 5-40°N) and the fractional contribution of ozone from (b) NHAF and (d) SHAF to the total African ozone over Asia (in %). The ozone values are the means from the 20-year GEOS-Chem simulation.
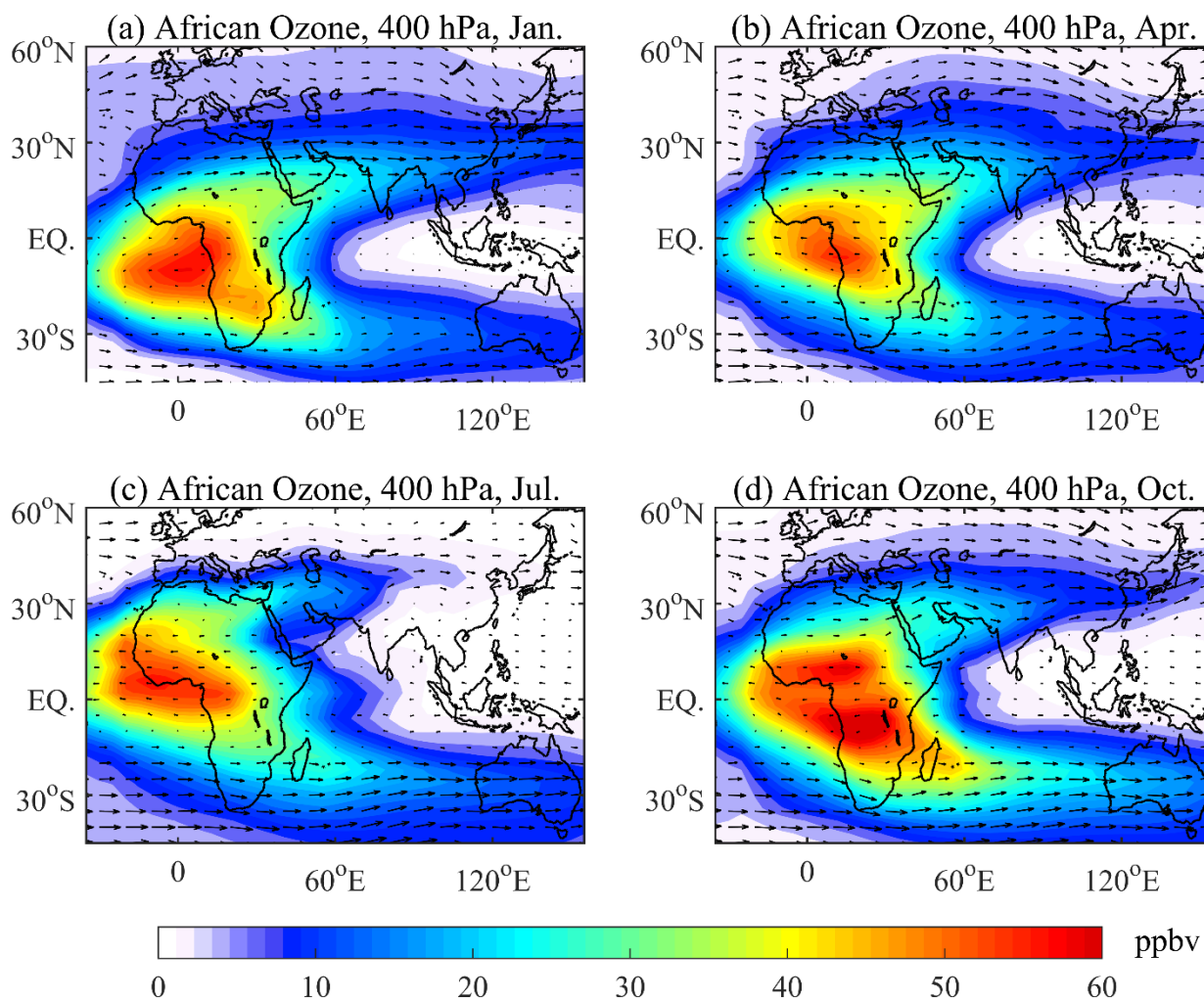
Figure 5. Horizontal distributions of African ozone (in ppbv, in color) overlaid with winds (in arrow) at 400 hPa in (a) January, (b) April, (c) July, and (d) October. The ozone values are the means from the 20-year GEOS-Chem simulation.
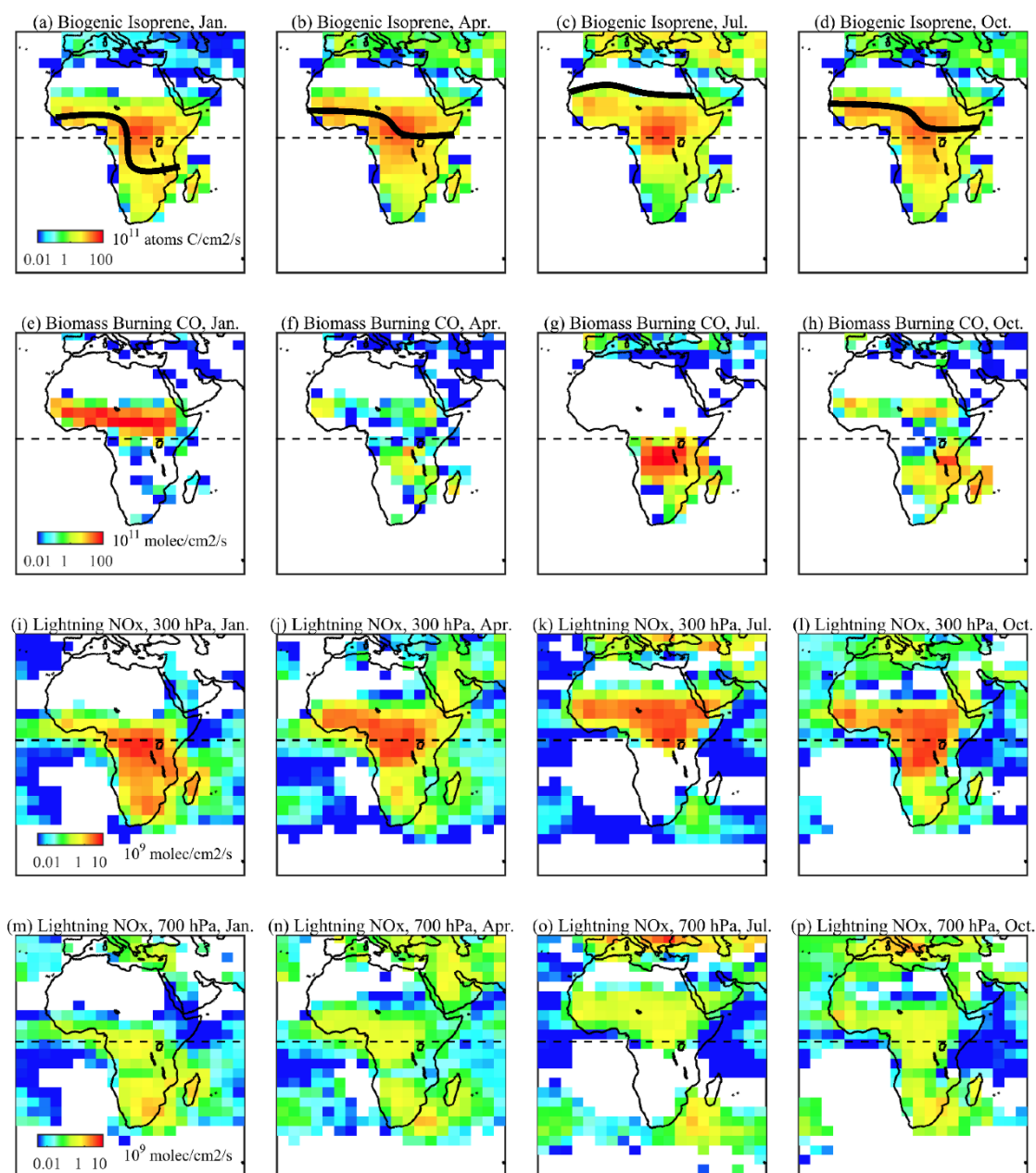
Figure 6. Distributions of isoprene emissions from biogenic sources (1st row), CO emissions from biomass burning (2nd row) and NO$_x$ emissions from lightning at 300 hPa (3rd row) and 700 hPa (4th row) by season in 2005. The data are based on the emission inventories in GEOS-Chem (see section 2.1 for details). The dash lines indicate the equator. The black solid lines in Figures 6a-6d indicate the location of the ITCZ.
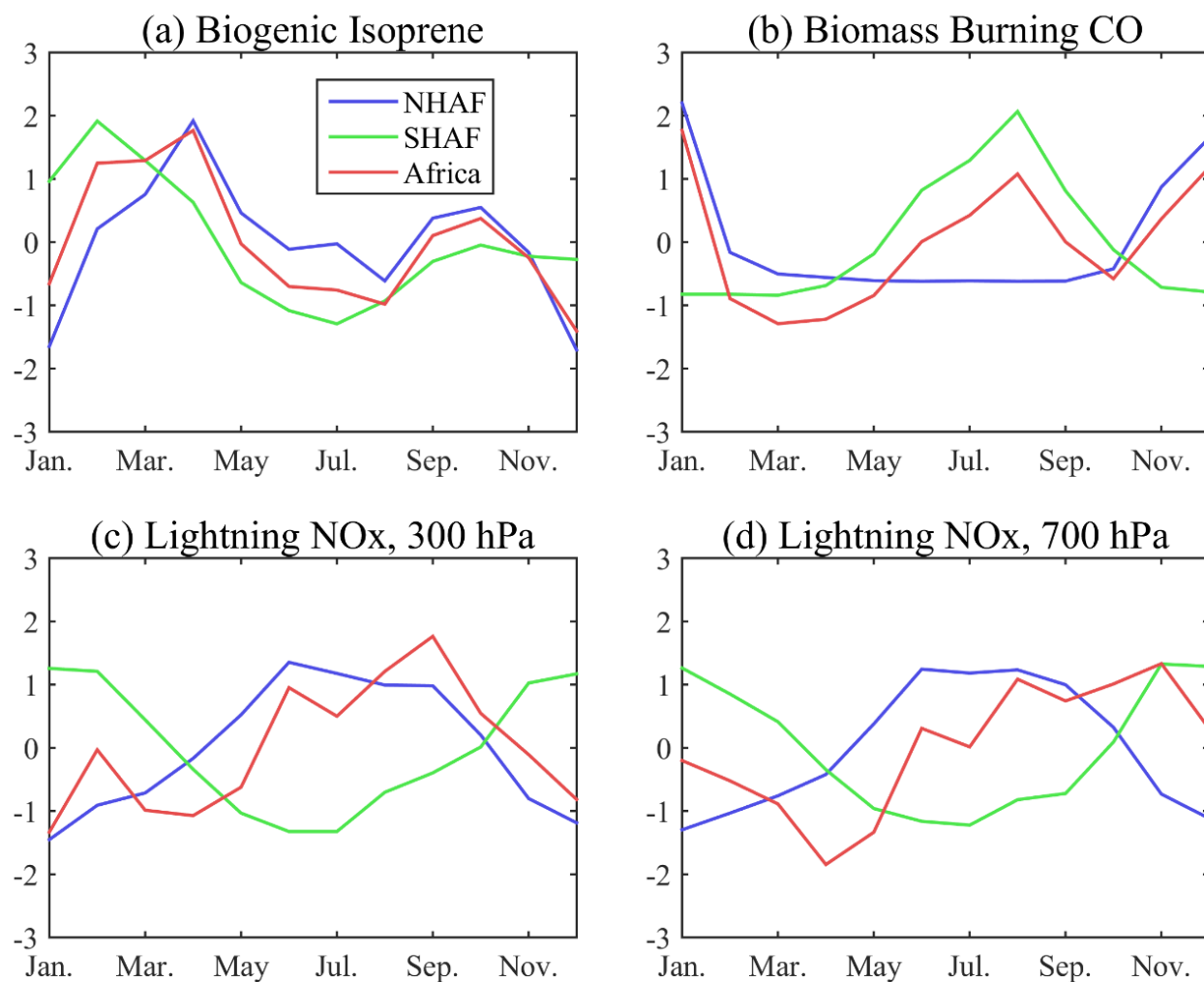
Figure 7. Seasonal variations of normalized values for isoprene emissions from (a) biogenic sources, (b) CO emissions from biomass burning, $NO_x$ emissions from lightning at (c) 300 hPa, and (d) 700 hPa averaged over Africa, NHAF and SHAF in 2005.
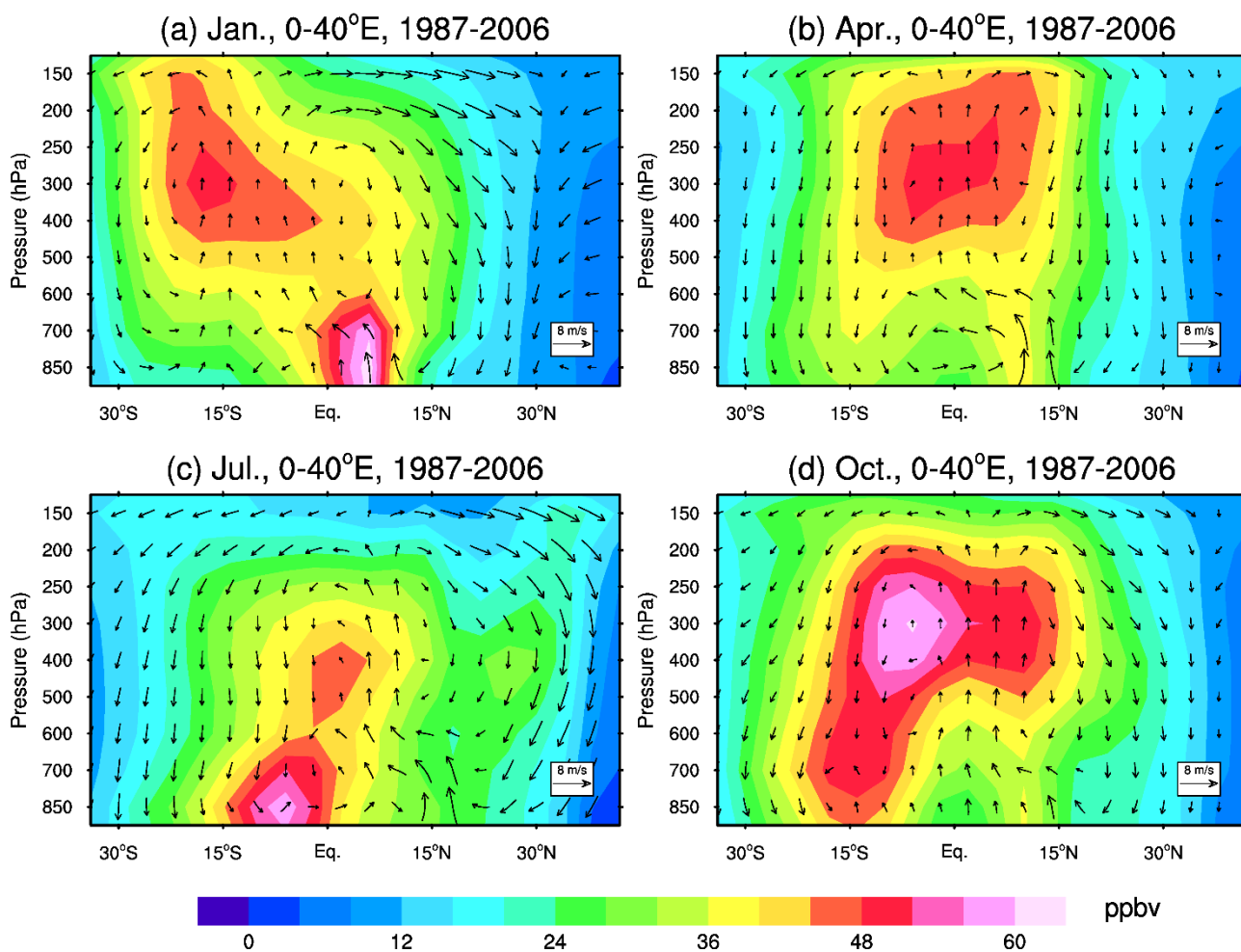
Figure 8. Latitude-altitude distribution of African ozone (in ppbv, in color), overlaid with winds (in arrow) in (a) January, (b) April, (c) July, and (d) October. The ozone values are the means over 0-40°E from the 20-year GEOS-Chem simulation. The vertical velocities in the p-coordinates are enlarged by 100 times for illustration purposes.
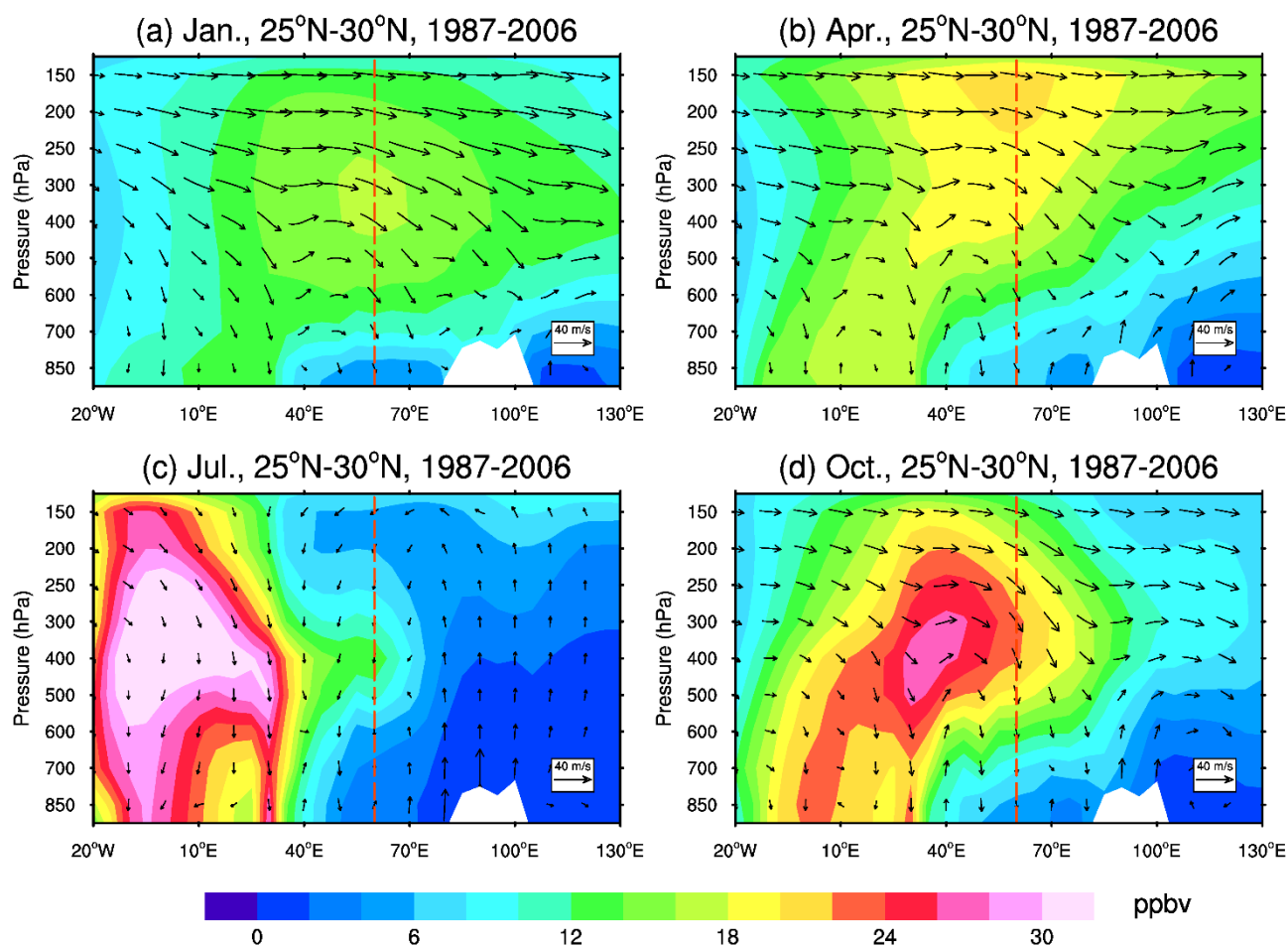
Figure 9. Longitude-altitude distribution of African ozone (in ppbv, in color), overlaid with winds (in arrow) in (a) January, (b) April, (c) July and (d) October. The ozone values are the means over 25°N-30°N from the 20-year GEOS-Chem simulation. White areas indicate topography. The red dash lines indicate the western border of Asia. The vertical velocities in the p-coordinates are enlarged by 100 times for illustration purposes.
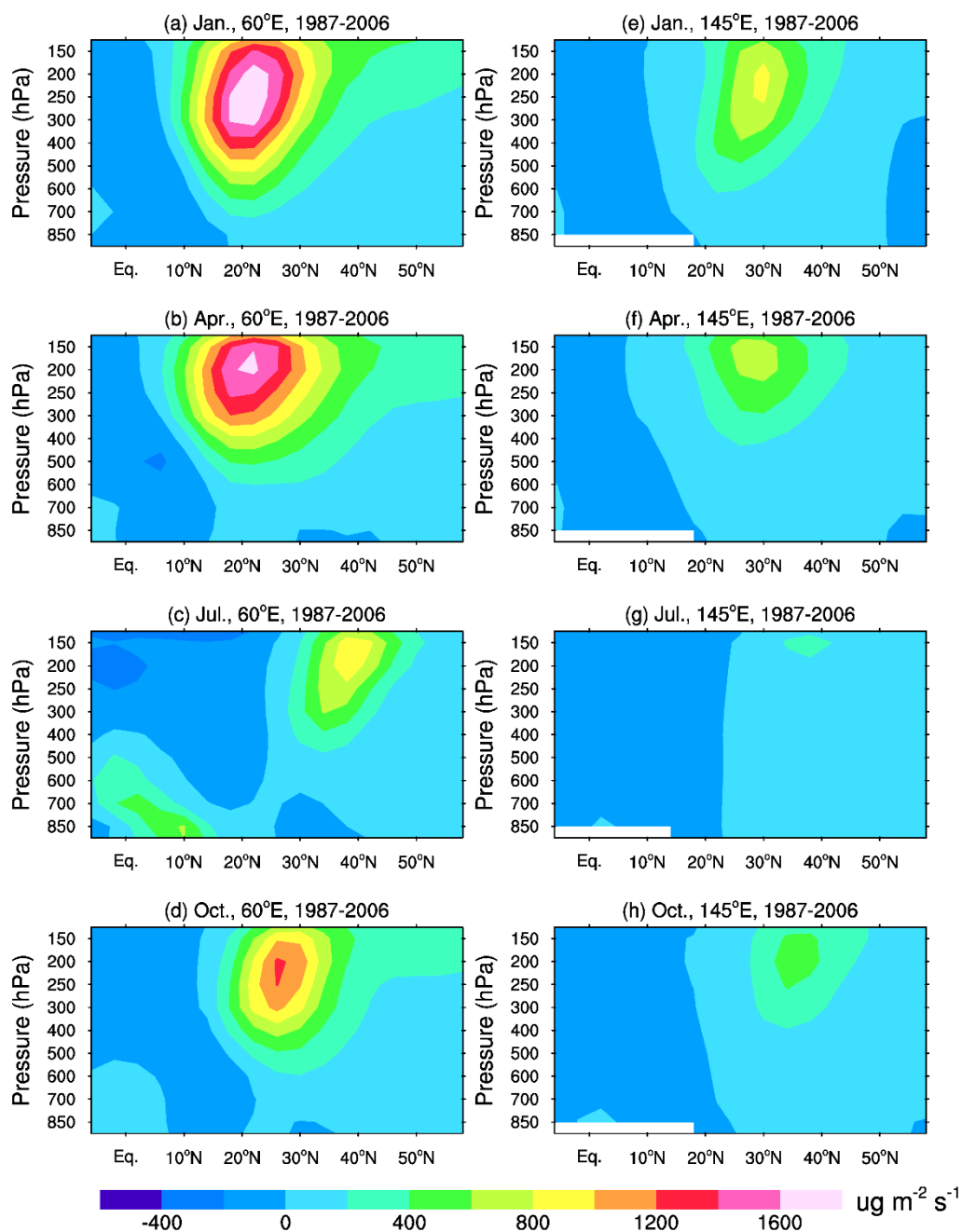
Figure 10. Latitude-altitude distribution of African ozone fluxes (in µg m$^{-2}$ s$^{-1}$) along the western border (60 °E, left panels) and eastern border (145 °E, right panels) of Asia in January (1$^{st}$ row), April (2$^{nd}$ row), July (3$^{rd}$ row) and October (4$^{th}$ row) averaged from 1987 to 2006.
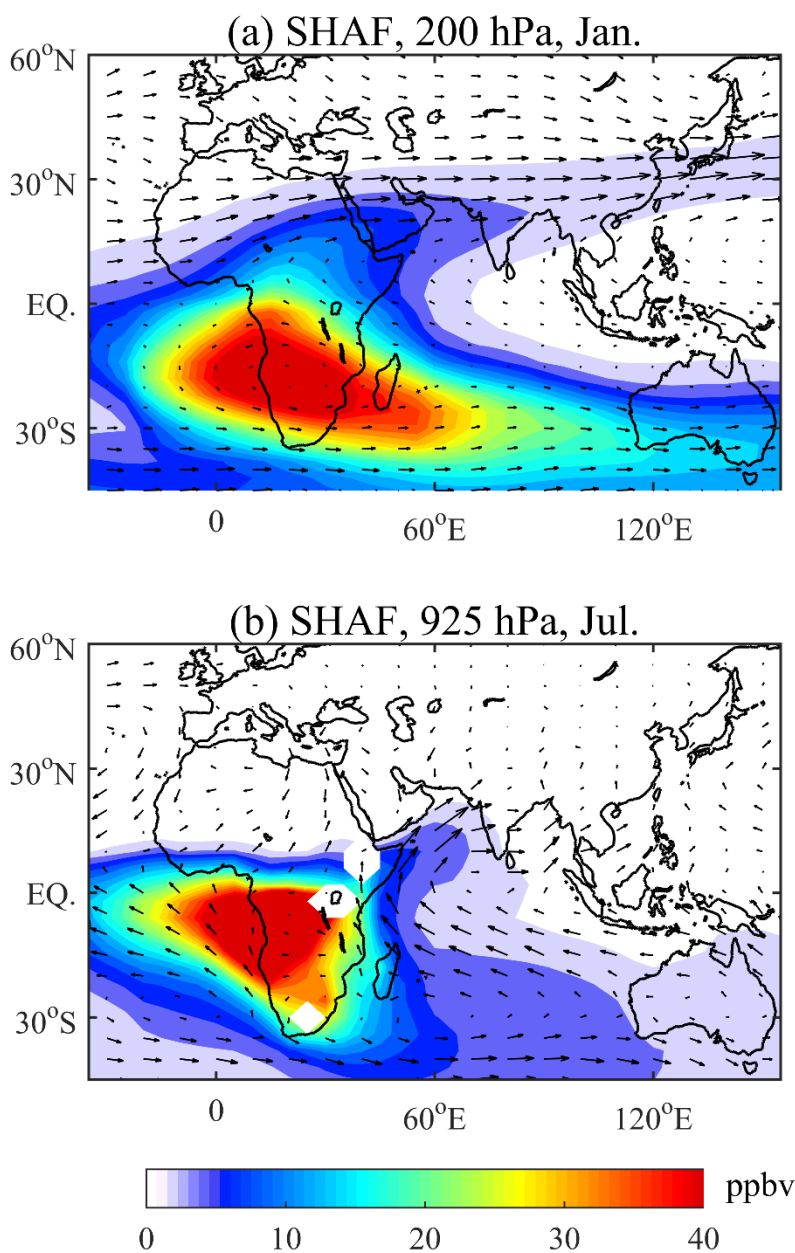
Figure 11. Distributions of ozone from SHAF (in ppbv, in color) overlaid with winds (in arrow) at (a) 200 hPa in January and (b) at 925 hPa in July. The ozone values are the means from the 20-year GEOS-Chem simulation.
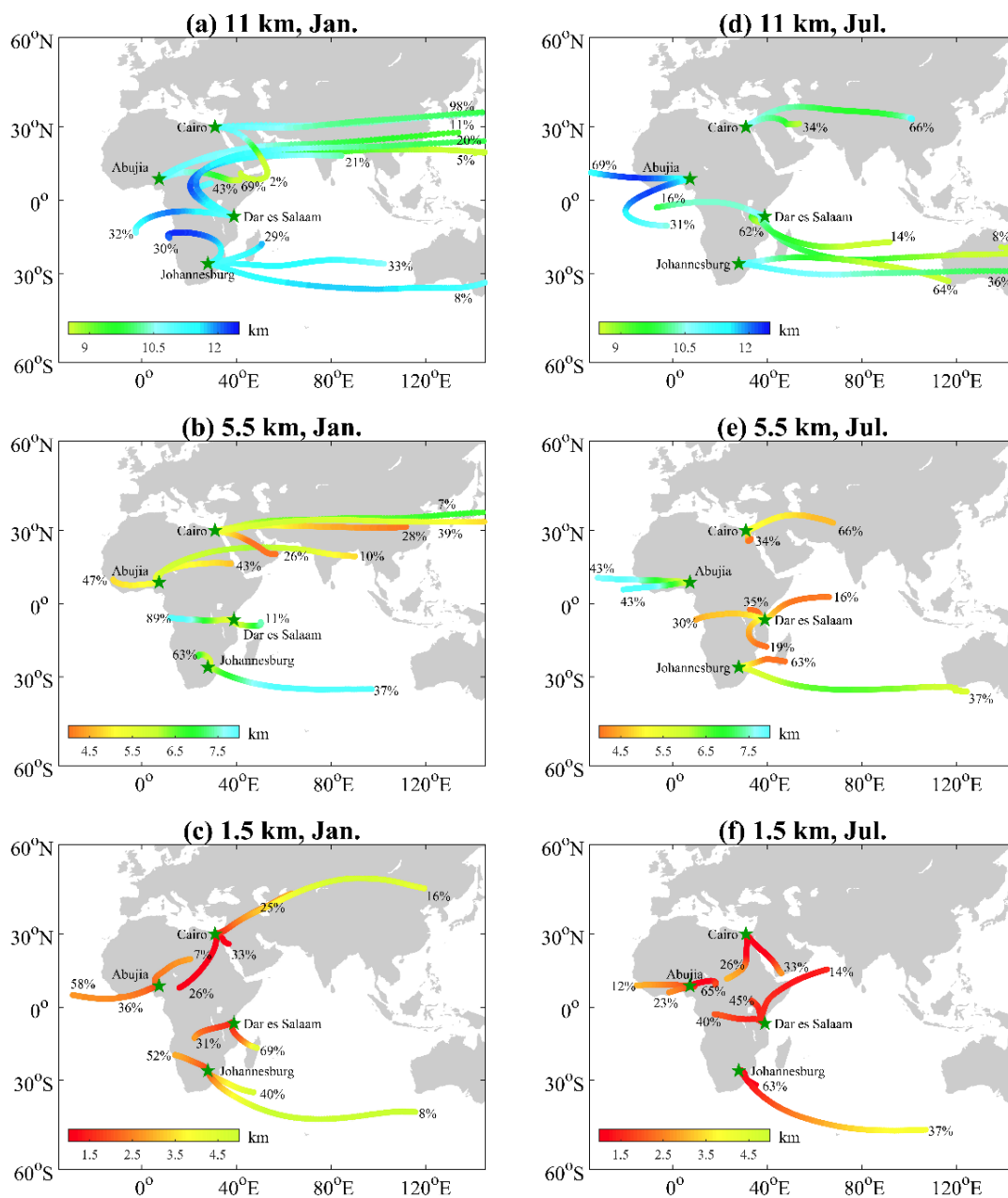
Figure 12. Six-day forward trajectories from Cairo (31$^o$E, 30$^o$N), Abuja (7.4$^o$E, 9$^o$N), Dar es Salaam (39$^o$E, 6.8$^o$S) and Johannesburg (28$^o$E, 26.2$^o$S) (stars) at 11 km (1$^{st}$ row), 5.5 km (2$^{nd}$ row), and 1.5 km (3$^{rd}$ row) in January (left panels) and July (right panels) clustered from 1987 to 2006.
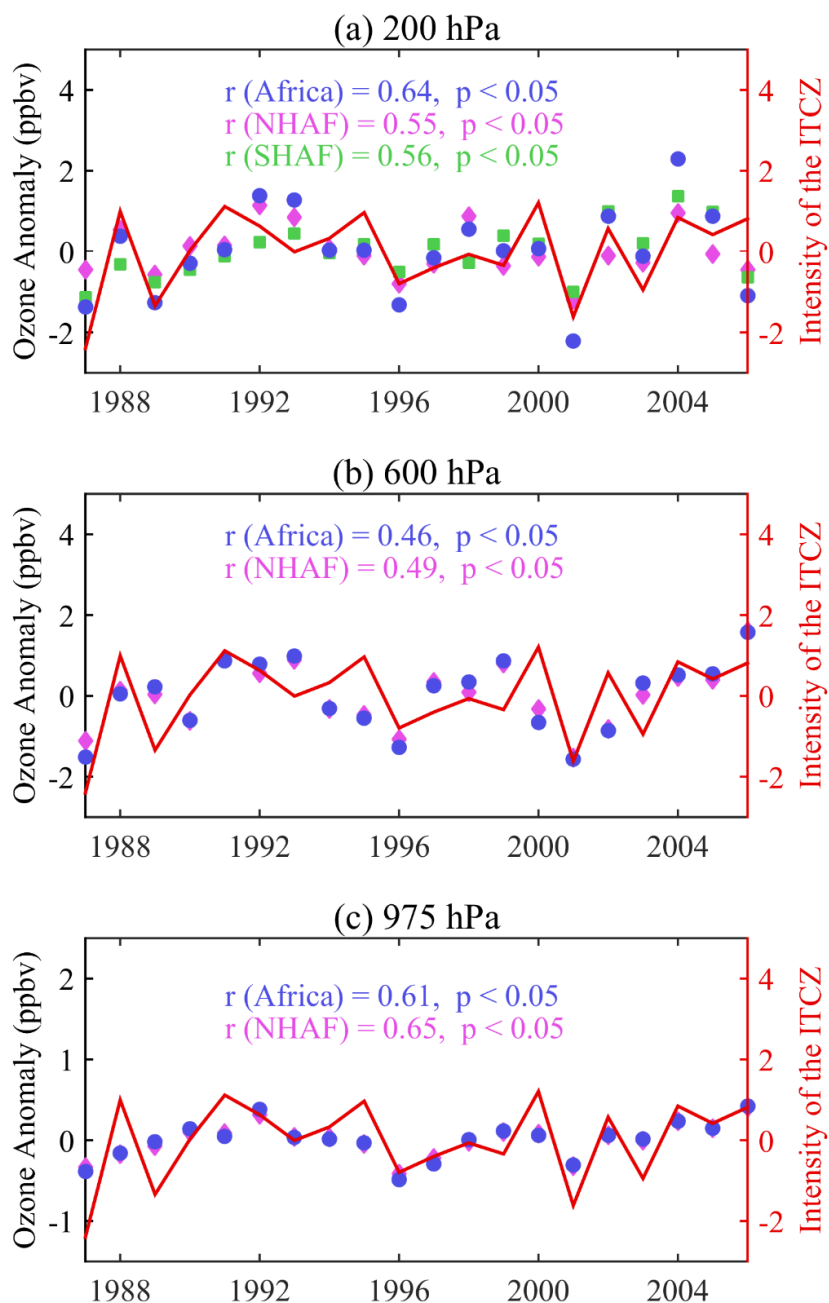
Figure 13. Interannual variation of the intensity of ITCZ (the values are normalized) over Africa and the anomaly of imported ozone from Africa, NHAF and SHAF over Asia from 1987 to 2006 at (a) 200 hPa, (b) 600 hPa, and (c) 975 hPa in January.
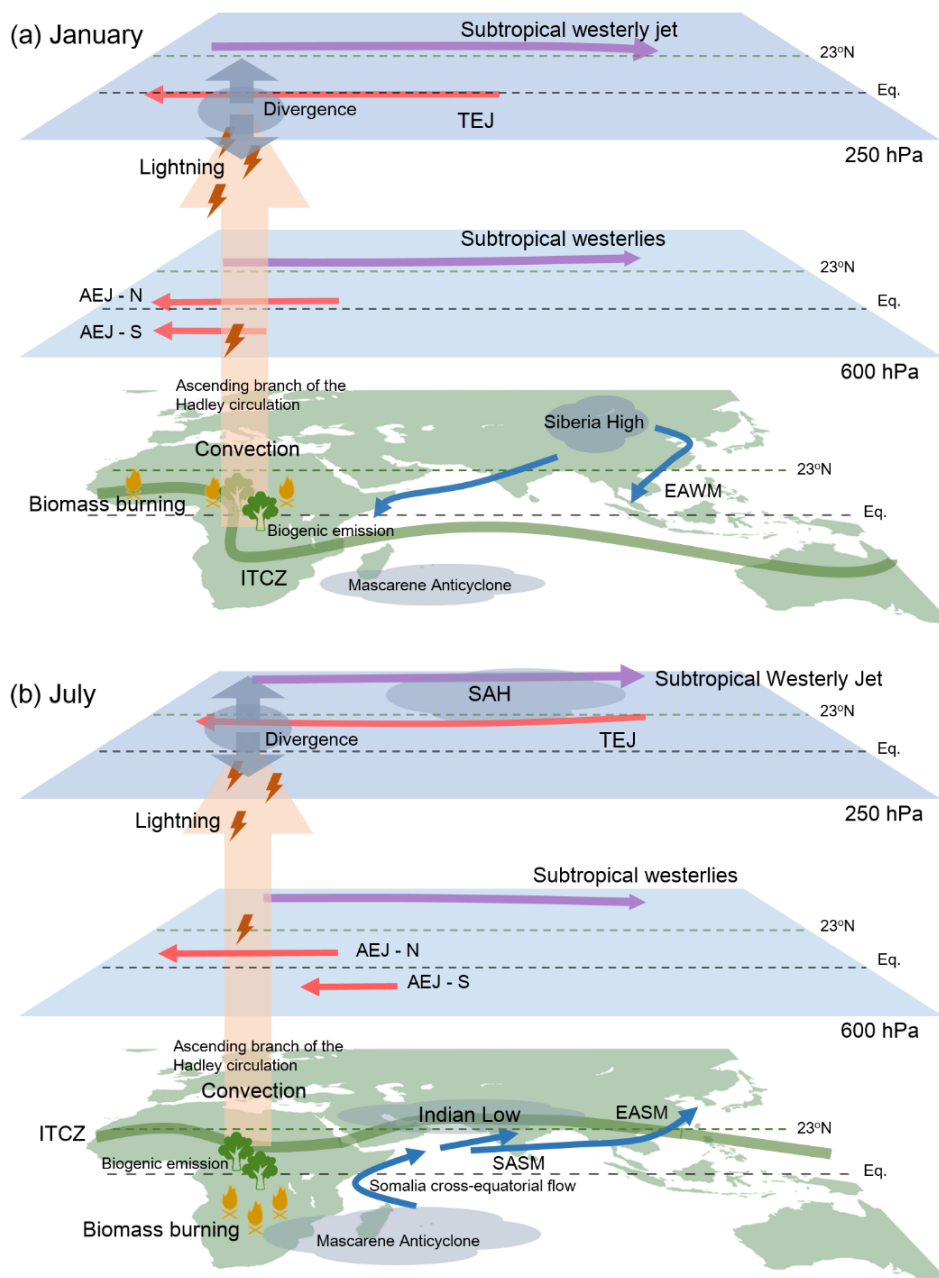
Figure 14. Schematic illustration of weather systems and the processes that impact the transport of African ozone to Asia in January (a) and July (b). TEJ stands for the tropical easterly jet. AEJ-N for the northern African easterly jet, AEJ-S for the southern African easterly jet, EAWM for the East Asian winter monsoon, EASM for the East Asian summer monsoon, SASM for the South Asian summer monsoon, SAH for the South Asian High, and ITCZ for the Intertropical Convergence Zone.